Finite element approximation of a vorticity formulation for the Oseen problem with variable viscosity

Verónica Anaya · Rubén Caraballo ·
Bryan Gómez-Vargas · David Mora ·
Ricardo Ruiz-Baier

Received: date / Revised version: date Updated: December 9, 2020

Abstract This paper deals with the analysis of an augmented mixed finite element method for the Oseen equations written in terms of velocity, vorticity, and pressure. The weak formulation is based on the introduction of least squares terms arising from the constitutive equation and from the incompressibility condition. We show that, under a CFL-type condition, the resulting augmented formulation satisfies the well-known Babuška-Brezzi theory. Next, repeating the arguments of the continuous analysis for the discrete case we show stability and solvability of the discrete problem. The method is suited for any Stokes inf-sup stable finite element pair for velocity and pressure, while for vorticity any generic discrete space (of arbitrary order) can be used. A priori and a posteriori error estimates are derived using as example two families of discrete subspaces. Finally, we provide a set of numerical tests illustrating the behaviour of the scheme, verifying the theoretical convergence rates, and showing the performance of the adaptive algorithm guided by residual a posteriori error estimation.

Keywords Oseen equations · velocity-vorticity-pressure formulation · mixed finite element methods · variable viscosity · a priori and a posteriori error analysis · adaptive mesh refinement

Mathematics Subject Classification (2000) 65N30 · 65N12 · 76D07 · 65N15

1 Introduction

Using vorticity as additional field in the formulation of incompressible flow equations can be advantageous in a number of applicative problems [51]. Starting from the seminal works [29,30] that focused on Stokes problems and where vorticity was sought in $\mathrm{H}(\mathbf{curl},\Omega)$, several different

V. Anaya · R. Caraballo · D. Mora
GIMNAP, Departamento de Matemática, Universidad del Bío-Bío, Casilla 5-C, Concepción, Chile.
E-mail: {vanaya,rcaraballo,dmora}@ubiobio.cl

B. Gómez-Vargas
Sección de Matemática, Sede de Occidente, Universidad de Costa Rica, San Ramón de Alajuela, Costa Rica.
E-mail: bryan.gomezvargas@ucr.ac.cr

D. Mora
CI^{2}MA, Universidad de Concepción, Casilla 160-C, Concepción, Chile.

R. Ruiz-Baier
School of Mathematical Sciences, Monash University, 9 Rainforest Walk, Melbourne VIC 3800, Australia.
E-mail: ricardo.ruizbaier@monash.edu

problems including Brinkman, Navier-Stokes, and related interface equations written in terms of vorticity have been studied from the viewpoint of numerical analysis of finite volume and mixed finite element methods exhibiting diverse properties and specific features. Some of these works include [2,3,4,9,8,27,14,49,50].

This paper addresses a formulation for Oseen equations and its mixed finite element discretisation, that are valid for the case of variable viscosity. This type of equations will appear, for instance, in the linearisation of non-Newtonian flow problems, as well as in applications where viscosity may depend on temperature, concentration or volume fractions, or other fields where the fluid flow patterns are strongly dependent on marked spatial distributions of viscosity [41, 45,46,48].

The specific literature related to the analysis of numerical schemes for the Oseen equations in terms of vorticity includes the non-conforming exponentially accurate least-squares spectral method proposed in [44], least-squares methods proposed in [52] for Oseen and Navier-Stokes equations with velocity boundary conditions, the family of vorticity-based first-order Oseen-type systems studied in [25], the enhanced accuracy formulation in terms of velocity-vorticity-helicity investigated in [13], and the recent mixed (exactly divergence-free) and DG discretisations for Oseen's problem in velocity-vorticity-pressure form given in [5]. However, in most of these references, the derivation of the variational formulations depends on the viscosity being constant. This is attributed to the fact that the usual vorticity-based weak formulation results from exploiting the following identity

$$\mathbf{curl}(\mathbf{curl}\, \boldsymbol{v}) = -\Delta \boldsymbol{v} + \nabla(\operatorname{div} \boldsymbol{v}), \tag{1.1}$$

applied to the viscous term. However the physically sensible friction term is $-\mathbf{div}(\nu\boldsymbol{\varepsilon}(\boldsymbol{u}))$, where $\boldsymbol{\varepsilon}(\boldsymbol{u})$ is the strain rate tensor (the symmetric gradient of the velocity field $\boldsymbol{u}$).

Extensions to cover the case of variable viscosity do exist in the literature. For instance, [31] addresses the well-posedness of the vorticity–velocity formulation of the Stokes problem with varying density and viscosity, and the equivalence of the vorticity–velocity and velocity–pressure formulations in appropriate functional spaces is proved. More recently, in [7] we have taken a different approach and employed an augmented vorticity-velocity-pressure formulation for Brinkman equations with variable viscosity. Here we extend that analysis to the generalised Oseen equations with variable viscosity, and address in particular how to deal with the additional challenges posed by the presence of the convective term that did not appear in the Brinkman momentum equation.

We will employ the so-called augmented formulations (also known as Galerkin least-squares methods), which can be regarded as a stabilisation technique where some terms are added to the variational formulation. Augmented finite elements have been considered in several works with applications in fluid mechanics (see, e.g., [6,10,11,15,24,20,21,22,38,47] and the references therein). These methods enjoy appealing advantages as those described in length in, e.g., [16,19], and reformulations of the set of equations following this approach are also of great importance in the design of block preconditioners (see [12,33] for an application in Oseen and Navier-Stokes equations in primal form, [34] for stress-velocity-pressure formulations for non-Newtonian flows, or [23,35] for stress-displacement-pressure mixed formulations for hyperelasticity). In the particular context of our mixed formulation for Oseen equations, the augmentation assists us in deriving the Babuška-Brezzi property of ellipticity on the kernel needed for the top-left diagonal block.

The formulation that we employ is non-symmetric, and the augmentation terms appear from least-squares contributions associated with the constitutive equation and the incompressibility constraint. The mixed variational formulation is shown to be well-posed under a condition on the viscosity bounds (a generalisation of the usual condition needed in Oseen equations, cf. Theorem 2.1 and Remark 2.2). Then we establish the well-posedness of the discrete problem for generic inf-sup stable finite elements (for velocity and pressure) in combination with a generic space for vorticity approximation. We obtain error estimates for two stable families of finite elements. We also derive a reliable and efficient residual-based a posteriori error estimator for the mixed problem, which can be fully computed locally.

The contents of the paper have been structured as follows. Functional spaces and recurrent notation will be collected in the remainder of this section. In Section 2 are presented the governing equations of the problem in terms of velocity, vorticity and pressure. In addition, we state our augmented formulation for the Oseen problem, and we perform the solvability analysis employing standard arguments from the Babuška–Brezzi theory. The finite element discretisation is presented in Section 3, where we also derive the stability analysis and optimal error estimates for two families of stable elements. In Section 4, we develop the a posteriori error analysis. Several numerical tests illustrating the convergence of the proposed method under different scenarios are reported in Section 5.

Preliminaries. Let Ω be a bounded domain of $\mathbb{R}^d$, $d = 2, 3$, with Lipschitz boundary $\Gamma = \partial\Omega$. For any $s \geq 0$, the notation $\|\cdot\|_{s,\Omega}$ stands for the norm of the Hilbertian Sobolev spaces $\mathrm{H}^s(\Omega)$ or $\mathrm{H}^s(\Omega)^d$, with the usual convention $\mathrm{H}^0(\Omega) := \mathrm{L}^2(\Omega)$.

Moreover, c and C, with or without subscripts, tildes, or hats, will represent a generic constant independent of the mesh parameter h, assuming different values in different occurrences. In addition, for any vector field $\boldsymbol{v} = (v_i)_{i=1}^d$ and any scalar field q we recall the notation:

$$\operatorname{div} \boldsymbol{v} = \sum_{i=1}^{d} \partial_i v_i, \;\; \mathbf{curl}\, \boldsymbol{v} = \begin{pmatrix} \partial_2 v_3 - \partial_3 v_2 \\ \partial_3 v_1 - \partial_1 v_3 \\ \partial_1 v_2 - \partial_2 v_1 \end{pmatrix}, \;\; \nabla q = \begin{pmatrix} \partial_1 q \\ \partial_2 q \\ \partial_3 q \end{pmatrix}.$$

Recall that, according to [39, Theorem 2.11], for a generic domain $\Omega \subseteq \mathbb{R}^3$, the relevant integration by parts formula corresponds to

$$\int_\Omega \mathbf{curl}\, \boldsymbol{\omega} \cdot \boldsymbol{v} = \int_\Omega \boldsymbol{\omega} \cdot \mathbf{curl}\, \boldsymbol{v} + \langle \boldsymbol{\omega} \times \boldsymbol{n}, \boldsymbol{v} \rangle_\Gamma,$$

which in 2D reads as

$$\int_\Omega \mathbf{curl}\, \omega \cdot \boldsymbol{v} = \int_\Omega \omega \operatorname{rot} \boldsymbol{v} - \langle \boldsymbol{v} \cdot \boldsymbol{t}, \omega \rangle_\Gamma, \tag{1.2}$$

with $\operatorname{rot} \boldsymbol{v} = \partial_1 v_2 - \partial_2 v_1$.

2 The model problem

Let us consider the well-known Oseen problem with non-constant viscosity modelling the steady-state flow of an incompressible viscous fluid. The governing equations can be stated, in terms of the velocity $\boldsymbol{u}$ and pressure p, as follows (see [39]):

$$\begin{aligned} \sigma \boldsymbol{u} - 2\,\mathbf{div}(\nu \boldsymbol{\varepsilon}(\boldsymbol{u})) + (\boldsymbol{\beta} \cdot \nabla)\boldsymbol{u} + \nabla p &= \boldsymbol{f} && \text{in } \Omega, && (2.1a) \\ \operatorname{div} \boldsymbol{u} &= 0 && \text{in } \Omega, && (2.1b) \\ \boldsymbol{u} &= \boldsymbol{0} && \text{on } \Gamma, && (2.1c) \\ (p, 1)_{0,\Omega} &= 0, && && (2.1d) \end{aligned}$$

where $\sigma > 0$ is inversely proportional to the time-step, $\boldsymbol{f} \in \mathrm{L}^2(\Omega)^d$ is a force density, $\boldsymbol{\beta} \in \mathrm{H}^1(\Omega)^d$ represents here an adequate approximation of velocity field (not necessarily divergence-free), and ν is the kinematic viscosity of the fluid satisfying: $\nu \in W^{1,\infty}(\Omega)$ and

$$0 < \nu_0 \leq \nu \leq \nu_1. \tag{2.2}$$

With the aim of proposing a vorticity-based formulation for the Oseen problem with variable viscosity, we consider the following identities

$$\begin{aligned}-2\mathbf{div}(\nu\boldsymbol{\varepsilon}(\boldsymbol{u})) &= -2\nu\mathbf{div}(\boldsymbol{\varepsilon}(\boldsymbol{u})) - 2\boldsymbol{\varepsilon}(\boldsymbol{u})\nabla\nu = -\nu\Delta\boldsymbol{u} - 2\boldsymbol{\varepsilon}(\boldsymbol{u})\nabla\nu \\ &= \nu\,\mathbf{curl}(\mathbf{curl}\,\boldsymbol{u}) - \nu\nabla(\operatorname{div}\boldsymbol{u}) - 2\boldsymbol{\varepsilon}(\boldsymbol{u})\nabla\nu.\end{aligned}$$

Therefore, we write the following version of the Oseen equations with variable viscosity where the unknowns are velocity $\boldsymbol{u}$, vorticity $\boldsymbol{\omega}$, and pressure p of the incompressible viscous fluid:

$$\sigma\boldsymbol{u} + \nu\,\mathbf{curl}\,\boldsymbol{\omega} - 2\boldsymbol{\varepsilon}(\boldsymbol{u})\nabla\nu + (\boldsymbol{\beta}\cdot\nabla)\boldsymbol{u} + \nabla p = \boldsymbol{f} \quad \text{in } \Omega, \tag{2.3a}$$

$$\boldsymbol{\omega} - \mathbf{curl}\,\boldsymbol{u} = \mathbf{0} \quad \text{in } \Omega, \tag{2.3b}$$

$$\operatorname{div}\boldsymbol{u} = 0 \quad \text{in } \Omega, \tag{2.3c}$$

$$\boldsymbol{u} = \mathbf{0} \quad \text{on } \Gamma, \tag{2.3d}$$

$$(p,1)_{0,\Omega} = 0, \tag{2.3e}$$

where we have considered the definition of the vorticity and have applied the incompressibility condition. The equations state, respectively, the momentum conservation, the constitutive relation, the mass balance, the no-slip boundary condition, and the pressure closure condition.

2.1 Variational formulation for the Oseen equations with non-constant viscosity

In this section, we propose a mixed variational formulation of system (2.3a)-(2.3e). First, we endow the space $\mathrm{H}_0^1(\Omega)^d$ with the following norm:

$$\|\boldsymbol{v}\|_{1,\Omega}^2 := \|\boldsymbol{v}\|_{0,\Omega}^2 + \|\,\mathbf{curl}\,\boldsymbol{v}\|_{0,\Omega}^2 + \|\operatorname{div}\boldsymbol{v}\|_{0,\Omega}^2,$$

and note that for $\mathrm{H}_0^1(\Omega)^d$ the above norm is equivalent to the usual norm. In particular, we have that there exists a positive constant C_{pf} such that:

$$\|\boldsymbol{v}\|_{1,\Omega}^2 \le C_{pf}(\|\,\mathbf{curl}\,\boldsymbol{v}\|_{0,\Omega}^2 + \|\operatorname{div}\boldsymbol{v}\|_{0,\Omega}^2) \qquad \forall \boldsymbol{v}\in \mathrm{H}_0^1(\Omega)^d,$$

where the above inequality is a consequence of the identity

$$\|\nabla\boldsymbol{v}\|_{0,\Omega}^2 = \|\,\mathbf{curl}\,\boldsymbol{v}\|_{0,\Omega}^2 + \|\operatorname{div}\boldsymbol{v}\|_{0,\Omega}^2, \tag{2.4}$$

which follows from (1.1) and the Poincaré inequality. Moreover, in order to establish a weak formulation for (2.3), we will use the following identity:

$$\mathbf{curl}(\phi\boldsymbol{v}) = \nabla\phi\times\boldsymbol{v} + \phi\,\mathbf{curl}\,\boldsymbol{v}, \tag{2.5}$$

valid for any vector field $\boldsymbol{v}$ and any scalar field ϕ.

After testing each equation of (2.3a)-(2.3d) against adequate functions, using (2.5), and imposing the boundary conditions, we end up with the following system:

$$\begin{aligned}\int_\Omega(\sigma\boldsymbol{u} + (\boldsymbol{\beta}\cdot\nabla)\boldsymbol{u})\cdot\boldsymbol{v} - 2\int_\Omega \boldsymbol{\varepsilon}(\boldsymbol{u})\nabla\nu\cdot\boldsymbol{v}& \\ + \int_\Omega \nu\boldsymbol{\omega}\cdot\mathbf{curl}\,\boldsymbol{v} + \int_\Omega \boldsymbol{\omega}\cdot(\nabla\nu\times\boldsymbol{v}) - \int_\Omega p\operatorname{div}\boldsymbol{v} &= \int_\Omega \boldsymbol{f}\cdot\boldsymbol{v}, \\ \int_\Omega \nu\boldsymbol{\theta}\cdot\mathbf{curl}\,\boldsymbol{u} - \int_\Omega \nu\boldsymbol{\omega}\cdot\boldsymbol{\theta} &= 0, \\ -\int_\Omega q\operatorname{div}\boldsymbol{u} &= 0,\end{aligned}$$

for all $(\boldsymbol{v},\boldsymbol{\theta},q)\in \mathrm{H}_0^1(\Omega)^d\times \mathrm{L}^2(\Omega)^{d(d-1)/2}\times \mathrm{L}_0^2(\Omega)$, where $\mathrm{L}_0^2(\Omega) := \{q\in \mathrm{L}^2(\Omega): (q,1)_{0,\Omega} = 0\}$.

Contrary to what is usually found in the the standard velocity-pressure mixed formulation, the ellipticity on the kernel condition for the Babuška-Brezzi theory is not straightforward in the above mixed formulation. Here is where the augmentation contributes to simplify the analysis. We introduce the following residual terms arising from equations (2.3b) and (2.3c):

$$\kappa_1\int_\Omega (\mathbf{curl}\,\boldsymbol{u}-\boldsymbol{\omega})\cdot\mathbf{curl}\,\boldsymbol{v} = 0 \qquad \forall \boldsymbol{v}\in \mathrm{H}_0^1(\Omega)^d, \tag{2.6a}$$

$$\kappa_2\int_\Omega \operatorname{div}\boldsymbol{u}\operatorname{div}\boldsymbol{v} = 0 \qquad \forall \boldsymbol{v}\in \mathrm{H}_0^1(\Omega)^d, \tag{2.6b}$$

where κ_1 and κ_2 are positive parameters to be specified later on.

In this way, we propose the following augmented variational formulation for (2.3):

Find $((\boldsymbol{u},\boldsymbol{\omega}),p)\in (\mathrm{H}_0^1(\Omega)^d\times \mathrm{L}^2(\Omega)^{d(d-1)/2})\times \mathrm{L}_0^2(\Omega)$ *such that*

$$A((\boldsymbol{u},\boldsymbol{\omega}),(\boldsymbol{v},\boldsymbol{\theta})) + B((\boldsymbol{v},\boldsymbol{\theta}),p) = F(\boldsymbol{v},\boldsymbol{\theta}) \qquad \forall (\boldsymbol{v},\boldsymbol{\theta})\in \mathrm{H}_0^1(\Omega)^d\times \mathrm{L}^2(\Omega)^{d(d-1)/2}, \tag{2.7a}$$

$$B((\boldsymbol{u},\boldsymbol{\omega}),q) = 0 \qquad \forall q\in \mathrm{L}_0^2(\Omega), \tag{2.7b}$$

where the bilinear forms and the linear functional are defined by

$$\begin{aligned} A((\boldsymbol{u},\boldsymbol{\omega}),(\boldsymbol{v},\boldsymbol{\theta})) &:= \int_\Omega (\sigma\boldsymbol{u}+(\boldsymbol{\beta}\cdot\nabla)\boldsymbol{u})\cdot\boldsymbol{v} + \int_\Omega \nu\boldsymbol{\omega}\cdot\boldsymbol{\theta} + \int_\Omega \nu\boldsymbol{\omega}\cdot\mathbf{curl}\,\boldsymbol{v} - \int_\Omega \nu\boldsymbol{\theta}\cdot\mathbf{curl}\,\boldsymbol{u} \\ &\quad + \kappa_1\int_\Omega \mathbf{curl}\,\boldsymbol{u}\cdot\mathbf{curl}\,\boldsymbol{v} + \kappa_2\int_\Omega \operatorname{div}\boldsymbol{u}\operatorname{div}\boldsymbol{v} - \kappa_1\int_\Omega \boldsymbol{\omega}\cdot\mathbf{curl}\,\boldsymbol{v} \\ &\quad - 2\int_\Omega \boldsymbol{\varepsilon}(\boldsymbol{u})\nabla\nu\cdot\boldsymbol{v} + \int_\Omega \boldsymbol{\omega}\cdot(\nabla\nu\times\boldsymbol{v}), \end{aligned} \tag{2.8a}$$

$$B((\boldsymbol{v},\boldsymbol{\theta}),q) := -\int_\Omega q\operatorname{div}\boldsymbol{v}, \tag{2.8b}$$

and

$$F(\boldsymbol{v},\boldsymbol{\theta}) := \int_\Omega \boldsymbol{f}\cdot\boldsymbol{v}, \tag{2.8c}$$

for all $(\boldsymbol{u},\boldsymbol{\omega}),(\boldsymbol{v},\boldsymbol{\theta})\in \mathrm{H}_0^1(\Omega)^d\times \mathrm{L}^2(\Omega)^{d(d-1)/2}$, and $q\in \mathrm{L}_0^2(\Omega)$.

As we will address in full detail in the next section, the proposed augmented mixed variational formulation will permit us to analyse the problem directly under the classical Babuška-Brezzi theory [19,37].

Remark 2.1 The above weak formulation has been written by considering a variable viscosity; however, it can be obviously used for constant viscosity.

2.2 Well-posedness analysis

In this section, we will address the well-posedness of the proposed weak formulation (2.7).

In our analysis, we will need to invoke the following inequality, which is a consequence of the Sobolev embedding $\mathrm{H}^1(\Omega)\hookrightarrow \mathrm{L}^4(\Omega)$

$$\left|\int_\Omega \operatorname{div}\boldsymbol{\beta}(\boldsymbol{u}\cdot\boldsymbol{v})\right| \le \widehat{C}\|\operatorname{div}\boldsymbol{\beta}\|_{0,\Omega}\|\boldsymbol{u}\|_{1,\Omega}\|\boldsymbol{v}\|_{1,\Omega}. \tag{2.9}$$

We will also make use of the following identity (cf. [39, Lemma 2.2])

$$\int_\Omega [(\boldsymbol{\beta}\cdot\nabla)\boldsymbol{u}]\cdot\boldsymbol{v} + \int_\Omega [(\boldsymbol{\beta}\cdot\nabla)\boldsymbol{v}]\cdot\boldsymbol{u} = -\int_\Omega \operatorname{div}\boldsymbol{\beta}(\boldsymbol{u}\cdot\boldsymbol{v}). \tag{2.10}$$

The continuity of the bilinear forms and the linear functional (cf. (2.8a)-(2.8c)), will be a consequence of the following lemma, whose proof follows standard arguments in combination with (2.2).

Lemma 2.1 *The following estimates hold*

$$\left|\sigma\int_\Omega \boldsymbol{u}\cdot\boldsymbol{v}\right| \le \sigma\|\boldsymbol{u}\|_{0,\Omega}\|\boldsymbol{v}\|_{0,\Omega}, \qquad \left|\int_\Omega \nu\boldsymbol{\omega}\cdot\boldsymbol{\theta}\right| \le \nu_1\|\boldsymbol{\omega}\|_{0,\Omega}\|\boldsymbol{\theta}\|_{0,\Omega},$$
$$\left|\int_\Omega [(\boldsymbol{\beta}\cdot\nabla)\boldsymbol{u}]\cdot\boldsymbol{v}\right| \le \widehat{C}|\!|\!|\boldsymbol{\beta}|\!|\!|_{1,\Omega}\|\nabla\boldsymbol{u}\|_{0,\Omega}|\!|\!|\boldsymbol{v}|\!|\!|_{1,\Omega},$$
$$\left|\int_\Omega \nu\boldsymbol{\theta}\cdot\mathbf{curl}\,\boldsymbol{v}\right| \le \nu_1\|\boldsymbol{\theta}\|_{0,\Omega}|\!|\!|\boldsymbol{v}|\!|\!|_{1,\Omega}, \qquad \left|\int_\Omega \boldsymbol{\varepsilon}(\boldsymbol{u})\nabla\nu\cdot\boldsymbol{v}\right| \le \|\nabla\nu\|_{\infty,\Omega}\|\boldsymbol{\varepsilon}(\boldsymbol{u})\|_{0,\Omega}\|\boldsymbol{v}\|_{0,\Omega},$$
$$\left|\int_\Omega \boldsymbol{\theta}\cdot(\nabla\nu\times\boldsymbol{v})\right| \le 2\|\nabla\nu\|_{\infty,\Omega}\|\boldsymbol{v}\|_{0,\Omega}\|\boldsymbol{\theta}\|_{0,\Omega}, \qquad |F(\boldsymbol{v},\boldsymbol{\theta})| \le \|\boldsymbol{f}\|_{0,\Omega}\|\boldsymbol{v}\|_{0,\Omega}.$$

As a consequence of the above lemma, we have that there exist positive constants $C_1, C_2, C_3 > 0$ such that

$$\begin{aligned}
|A((\boldsymbol{u},\boldsymbol{\omega}),(\boldsymbol{v},\boldsymbol{\theta}))| &\le C_1\|(\boldsymbol{u},\boldsymbol{\omega})\|\|(\boldsymbol{v},\boldsymbol{\theta})\|,\\
|B((\boldsymbol{v},\boldsymbol{\theta}),q)| &\le C_2\|(\boldsymbol{v},\boldsymbol{\theta})\|\|q\|_{0,\Omega},\\
|F(\boldsymbol{v},\boldsymbol{\theta})| &\le C_3\|(\boldsymbol{v},\boldsymbol{\theta})\|,
\end{aligned}$$

with the product space norm defined as

$$\|(\boldsymbol{v},\boldsymbol{\theta})\|^2 := |\!|\!|\boldsymbol{v}|\!|\!|_{1,\Omega}^2 + \|\boldsymbol{\theta}\|_{0,\Omega}^2.$$

The following lemma states the ellipticity of the bilinear form $A(\cdot,\cdot)$.

Lemma 2.2 *Assuming that*

$$\sigma > \frac{9\|\nabla\nu\|_{\infty,\Omega}^2}{\nu_0} \qquad \text{and} \qquad \widehat{C}\|\operatorname{div}\boldsymbol{\beta}\|_{0,\Omega} < \min\left\{\sigma - \frac{9\|\nabla\nu\|_{\infty,\Omega}^2}{\nu_0}, \frac{\nu_0}{12}\right\}. \tag{2.11}$$

If we chose $\kappa_1 = \frac{2}{3}\nu_0$ and $\kappa_2 > \dfrac{\nu_0}{3}$. Then, there exists a constant $\alpha > 0$ such that

$$A((\boldsymbol{v},\boldsymbol{\theta}),(\boldsymbol{v},\boldsymbol{\theta})) \ge \alpha\|(\boldsymbol{v},\boldsymbol{\theta})\|^2 \qquad \forall (\boldsymbol{v},\boldsymbol{\theta}) \in \mathrm{H}_0^1(\Omega)^d \times \mathrm{L}^2(\Omega)^{d(d-1)/2}.$$

Proof Let $(\boldsymbol{v},\boldsymbol{\theta}) \in \mathrm{H}_0^1(\Omega)^d \times \mathrm{L}^2(\Omega)^{d(d-1)/2}$. As a consequence of Lemma 2.1, we have that

$$\begin{aligned}
\left|2\int_\Omega \boldsymbol{\varepsilon}(\boldsymbol{v})\nabla\nu\cdot\boldsymbol{v}\right| &\le 2\|\nabla\nu\|_{\infty,\Omega}\left(\frac{\nu_0}{12\|\nabla\nu\|_{\infty,\Omega}}\|\nabla\boldsymbol{v}\|_{0,\Omega}^2 + \frac{3\|\nabla\nu\|_{\infty,\Omega}}{\nu_0}\|\boldsymbol{v}\|_{0,\Omega}^2\right)\\
&= \frac{\nu_0}{6}(\|\mathbf{curl}\,\boldsymbol{v}\|_{0,\Omega}^2 + \|\operatorname{div}\boldsymbol{v}\|_{0,\Omega}^2) + \frac{6\|\nabla\nu\|_{\infty,\Omega}^2}{\nu_0}\|\boldsymbol{v}\|_{0,\Omega}^2,
\end{aligned} \tag{2.12}$$

where we have used (2.4). Moreover, using that $\|(\nabla\nu\times\boldsymbol{v})\|_{0,\Omega} \le 2\|\nabla\nu\|_{\infty,\Omega}\|\boldsymbol{v}\|_{0,\Omega}$, we get

$$\left|\int_\Omega \boldsymbol{\theta}\cdot(\nabla\nu\times\boldsymbol{v})\right| \le 2\|\nabla\nu\|_{\infty,\Omega}\left(\frac{\nu_0}{6\|\nabla\nu\|_{\infty,\Omega}}\|\boldsymbol{\theta}\|_{0,\Omega}^2 + \frac{3\|\nabla\nu\|_{\infty,\Omega}}{2\nu_0}\|\boldsymbol{v}\|_{0,\Omega}^2\right)$$

$$
\begin{aligned}
&= \frac{\nu_0}{3}\|\boldsymbol{\theta}\|_{0,\Omega}^2 + \frac{3\|\nabla\nu\|_{\infty,\Omega}^2}{\nu_0}\|\boldsymbol{v}\|_{0,\Omega}^2, \\
\left|\kappa_1\int_\Omega \boldsymbol{\theta}\cdot\mathbf{curl}\,\boldsymbol{v}\right| &\leq \kappa_1\left(\frac{\nu_0}{3\kappa_1}\|\boldsymbol{\theta}\|_{0,\Omega}^2 + \frac{3\kappa_1}{4\nu_0}\|\,\mathbf{curl}\,\boldsymbol{v}\|_{0,\Omega}^2\right) \\
&= \frac{\nu_0}{3}\|\boldsymbol{\theta}\|_{0,\Omega}^2 + \frac{3\kappa_1^2}{4\nu_0}\|\,\mathbf{curl}\,\boldsymbol{v}\|_{0,\Omega}^2. \qquad (2.13)
\end{aligned}
$$

Thus, using the Cauchy-Schwarz inequality, (2.12)-(2.13), (2.10) and (2.9), we obtain

$$
\begin{aligned}
A((\boldsymbol{v},\boldsymbol{\theta}),(\boldsymbol{v},\boldsymbol{\theta})) \geq& \sigma\|\boldsymbol{v}\|_{0,\Omega}^2 + \int_\Omega [(\boldsymbol{\beta}\cdot\nabla)\boldsymbol{v}]\cdot\boldsymbol{v} + \int_\Omega \nu|\boldsymbol{\theta}|^2 + \kappa_1\|\,\mathbf{curl}\,\boldsymbol{v}\|_{0,\Omega}^2 + \kappa_2\|\operatorname{div}\boldsymbol{v}\|_{0,\Omega}^2 \\
&- \kappa_1\int_\Omega \boldsymbol{\theta}\cdot\mathbf{curl}\,\boldsymbol{v} - 2\int_\Omega \boldsymbol{\varepsilon}(\boldsymbol{v})\nabla\nu\cdot\boldsymbol{v} + \int_\Omega \boldsymbol{\theta}\cdot(\nabla\nu\times\boldsymbol{v}) \\
\geq& \sigma\|\boldsymbol{v}\|_{0,\Omega}^2 - \widehat{C}\|\operatorname{div}\boldsymbol{\beta}\|_{0,\Omega}\|\boldsymbol{v}\|_{1,\Omega}^2 + \nu_0\|\boldsymbol{\theta}\|_{0,\Omega}^2 + \kappa_1\|\,\mathbf{curl}\,\boldsymbol{v}\|_{0,\Omega}^2 + \kappa_2\|\operatorname{div}\boldsymbol{v}\|_{0,\Omega}^2 \\
&- \frac{\nu_0}{3}\|\boldsymbol{\theta}\|_{0,\Omega}^2 - \frac{3\kappa_1^2}{4\nu_0}\|\,\mathbf{curl}\,\boldsymbol{v}\|_{0,\Omega}^2 - \frac{\nu_0}{6}(\|\,\mathbf{curl}\,\boldsymbol{v}\|_{0,\Omega}^2 + \|\operatorname{div}\boldsymbol{v}\|_{0,\Omega}^2) \\
&- \frac{6\|\nabla\nu\|_{\infty,\Omega}^2}{\nu_0}\|\boldsymbol{v}\|_{0,\Omega}^2 - \frac{\nu_0}{3}\|\boldsymbol{\theta}\|_{0,\Omega}^2 - \frac{3\|\nabla\nu\|_{\infty,\Omega}^2}{\nu_0}\|\boldsymbol{v}\|_{0,\Omega}^2 \\
=& \frac{\nu_0}{3}\|\boldsymbol{\theta}\|_{0,\Omega}^2 + \left(\kappa_1 - \frac{3\kappa_1^2}{4\nu_0} - \frac{\nu_0}{6} - \widehat{C}\|\operatorname{div}\boldsymbol{\beta}\|_{0,\Omega}\right)\|\,\mathbf{curl}\,\boldsymbol{v}\|_{0,\Omega}^2 \\
&+ \left(\kappa_2 - \frac{\nu_0}{6} - \widehat{C}\|\operatorname{div}\boldsymbol{\beta}\|_{0,\Omega}\right)\|\operatorname{div}\boldsymbol{v}\|_{0,\Omega}^2 \\
&+ (\sigma - \frac{9\|\nabla\nu\|_{\infty,\Omega}^2}{\nu_0} - \widehat{C}\|\operatorname{div}\boldsymbol{\beta}\|_{0,\Omega})\|\boldsymbol{v}\|_{0,\Omega}^2 \\
=& \frac{\nu_0}{3}\|\boldsymbol{\theta}\|_{0,\Omega}^2 + \left(\frac{\nu_0}{6} - \widehat{C}\|\operatorname{div}\boldsymbol{\beta}\|_{0,\Omega}\right)\|\,\mathbf{curl}\,\boldsymbol{v}\|_{0,\Omega}^2 \\
&+ \left(\kappa_2 - \frac{\nu_0}{6} - \widehat{C}\|\operatorname{div}\boldsymbol{\beta}\|_{0,\Omega}\right)\|\operatorname{div}\boldsymbol{v}\|_{0,\Omega}^2 \\
&+ \left(\sigma - \frac{9\|\nabla\nu\|_{\infty,\Omega}^2}{\nu_0} - \widehat{C}\|\operatorname{div}\boldsymbol{\beta}\|_{0,\Omega}\right)\|\boldsymbol{v}\|_{0,\Omega}^2.
\end{aligned}
$$

Now, using assumption (2.11), we have

$$
A((\boldsymbol{v},\boldsymbol{\theta}),(\boldsymbol{v},\boldsymbol{\theta})) \geq \alpha\|(\boldsymbol{v},\boldsymbol{\theta})\|^2,
$$

where

$$
\alpha := \min\left\{\frac{\nu_0}{3}, \frac{\nu_0}{6} - \widehat{C}\|\operatorname{div}\boldsymbol{\beta}\|_{0,\Omega}, \kappa_2 - \frac{\nu_0}{6} - \widehat{C}\|\operatorname{div}\boldsymbol{\beta}\|_{0,\Omega}, \sigma - \frac{9\|\nabla\nu\|_{0,\Omega}^2}{\nu_0} - \widehat{C}\|\operatorname{div}\boldsymbol{\beta}\|_{0,\Omega}\right\},
$$

which is clearly positive according to (2.11) and the assumptions on κ_1 and κ_2, concluding the proof. □

Now we recall the following result related to the inf-sup condition: There exists $C > 0$, depending only on Ω, such that (cf. [37])

$$
\sup_{0\neq\boldsymbol{v}\in\mathrm{H}_0^1(\Omega)^d} \frac{\left|\int_\Omega q\operatorname{div}\boldsymbol{v}\right|}{\|\boldsymbol{v}\|_{1,\Omega}} \geq C\|q\|_{0,\Omega} \quad \forall q\in\mathrm{L}_0^2(\Omega).
$$

As a consequence, we immediately have the following lemma.

Lemma 2.3 *There exists $\gamma > 0$, independent of ν, such that*

$$\sup_{0 \neq (\boldsymbol{v},\boldsymbol{\theta}) \in \mathrm{H}_0^1(\Omega)^d \times \mathrm{L}^2(\Omega)^{d(d-1)/2}} \frac{|B((\boldsymbol{v},\boldsymbol{\theta}),q)|}{\|(\boldsymbol{v},\boldsymbol{\theta})\|} \geq \gamma \|q\|_{0,\Omega} \quad \forall q \in \mathrm{L}_0^2(\Omega).$$

We state the well-posedness of problem (2.7) in the next theorem.

Theorem 2.1 *Assume that the hypotheses of Lemma 2.2 hold true. Then, there exists a unique solution $((\boldsymbol{u},\boldsymbol{\omega}),p) \in (\mathrm{H}_0^1(\Omega)^d \times \mathrm{L}^2(\Omega)^{d(d-1)/2}) \times \mathrm{L}_0^2(\Omega)$ to problem (2.7). Moreover, there exists $C > 0$ such that*

$$\|(\boldsymbol{u},\boldsymbol{\omega})\| + \|p\|_{0,\Omega} \leq C\|\boldsymbol{f}\|_{0,\Omega}.$$

Proof The proof follows from Lemmas 2.2 and 2.3, and a direct consequence of the Babuška-Brezzi Theorem ([19, Theorem II.1.1]). □

Remark 2.2 If in the Oseen problem (2.7), the given convective velocity field $\boldsymbol{\beta} \in \mathrm{H}^1(\Omega)^d$ satisfies in addition that $\operatorname{div}\boldsymbol{\beta} = 0$ in Ω (solenoidal), then, problem (2.7) is well-posed under the assumption

$$\sigma\nu_0 > 9\|\nabla\nu\|_{\infty,\Omega}^2, \tag{2.14}$$

and where we choose $\kappa_1 = \frac{2}{3}\nu_0$ and $\kappa_2 > \dfrac{\nu_0}{3}$.

Remark 2.3 Assumptions (2.11) or (2.14) hold provided one selects σ appropriately. As this parameter represents the inverse of the timestep (whenever Oseen is derived as a time discretisation of Navier-Stokes), the aforementioned relation can be regarded as a CFL-type condition.

Remark 2.4 Notice that the unique solution of (2.7) is certainly the solution of system (2.3a)-(2.3e). This fact is employed later on in Section 4 to prove the efficiency of the proposed a posteriori error estimator.

3 Numerical discretisation

In this section, we will construct a finite element scheme associated with (2.7), we will consider generic finite element subspaces yielding the unique solvability of the discrete scheme. We will also derive the a priori error estimates, and provide the corresponding rates of convergence for the different methods cover by our analysis.

Let $\{\mathcal{T}_h(\Omega)\}_{h>0}$ be a shape-regular family of partitions of the polygonal/polyhedral region $\bar{\Omega}$, by triangles/tetrahedrons T of diameter h_T, with meshsize $h := \max\{h_T : T \in \mathcal{T}_h(\Omega)\}$. In what follows, given an integer $k \geq 0$ and a subset S of $\mathbb{R}^d$, $\mathbb{P}_k(S)$ denotes the space of polynomial functions defined on S and being of degree $\leq k$.

Now, we consider generic finite dimensional subspaces $\mathbf{V}_h \subseteq \mathrm{H}_0^1(\Omega)^d$, $\mathbf{W}_h \subseteq \mathrm{L}^2(\Omega)^{d(d-1)/2}$ and $Q_h \subseteq \mathrm{L}_0^2(\Omega)$ such that the following discrete inf-sup holds

$$\sup_{0 \neq (\boldsymbol{v}_h,\boldsymbol{\theta}_h) \in \mathbf{V}_h \times \mathbf{W}_h} \frac{|B((\boldsymbol{v}_h,\boldsymbol{\theta}_h),q_h)|}{\|(\boldsymbol{v}_h,\boldsymbol{\theta}_h)\|} \geq \gamma_0 \|q_h\|_{0,\Omega} \quad \forall q_h \in Q_h, \tag{3.1}$$

where $\gamma_0 > 0$ is independent of h.

In this way, the above inf-sup condition can be obtained if $(\mathbf{V}_h, Q_h)$ is an inf-sup stable pair for the classical Stokes problem. Moreover, the discrete space $\mathbf{W}_h \subseteq \mathrm{L}^2(\Omega)^{d(d-1)/2}$ for the vorticity can be taken as continuous or discontinuous polynomial space. Here we will consider both options.

Now, we are in a position to introduce the finite element scheme related to problem (2.7).

Find $((\boldsymbol{u}_h, \boldsymbol{\omega}_h), p_h) \in (\mathbf{V}_h \times \mathbf{W}_h) \times Q_h$ *such that*

$$\begin{aligned} A((\boldsymbol{u}_h, \boldsymbol{\omega}_h), (\boldsymbol{v}_h, \boldsymbol{\theta}_h)) + B((\boldsymbol{v}_h, \boldsymbol{\theta}_h), p_h) &= F(\boldsymbol{v}_h, \boldsymbol{\theta}_h) \qquad \forall (\boldsymbol{v}_h, \boldsymbol{\theta}_h) \in \mathbf{V}_h \times \mathbf{W}_h, \\ B((\boldsymbol{u}_h, \boldsymbol{\omega}_h), q_h) &= 0 \qquad\qquad\quad\; \forall q \in Q_h. \end{aligned} \tag{3.2}$$

The next step is to establish the unique solvability and convergence of the discrete problem (3.2).

Theorem 3.1 *Assume that the hypotheses of Lemma 2.2 hold true. Let* $\mathbf{V}_h \subseteq \mathrm{H}_0^1(\Omega)^d$, $\mathbf{W}_h \subseteq \mathrm{L}^2(\Omega)^{d(d-1)/2}$ *and* $Q_h \subseteq \mathrm{L}_0^2(\Omega)$ *such that* (3.1) *holds true. Then, there exists a unique* $((\boldsymbol{u}_h, \boldsymbol{\omega}_h), p_h) \in (\mathbf{V}_h \times \mathbf{W}_h) \times Q_h$ *solution of the Galerkin scheme* (3.2)*. Moreover, there exist positive constants* $\hat{C}_1$, $\hat{C}_2 > 0$*, independent of* h*, such that*

$$\|(\boldsymbol{u}_h, \boldsymbol{\omega}_h)\| + \|p_h\|_{0,\Omega} \leq \hat{C}_1 \|\boldsymbol{f}\|_{0,\Omega}, \tag{3.3a}$$

and

$$\begin{aligned} &\|(\boldsymbol{u}, \boldsymbol{\omega}) - (\boldsymbol{u}_h, \boldsymbol{\omega}_h)\| + \|p - p_h\|_{0,\Omega} \\ &\qquad \leq \hat{C}_2 \inf_{(\boldsymbol{v}_h, \boldsymbol{\theta}_h, q_h) \in \mathbf{V}_h \times \mathbf{W}_h \times \mathrm{Q}_h} (\|\!|\boldsymbol{u} - \boldsymbol{v}_h|\!\|_{1,\Omega} + \|\boldsymbol{\omega} - \boldsymbol{\theta}_h\|_{0,\Omega} + \|p - q_h\|_{0,\Omega}), \end{aligned} \tag{3.3b}$$

where $((\boldsymbol{u}, \boldsymbol{\omega}), p) \in (\mathrm{H}_0^1(\Omega)^d \times \mathrm{L}^2(\Omega)^{d(d-1)/2}) \times \mathrm{L}_0^2(\Omega)$ *is the unique solution of* (2.7)*.*

3.1 Discrete subspaces and error estimates

In this section, we will define explicit families of finite element subspaces yielding the unique solvability of the discrete scheme (3.2). In addition, we derive the corresponding rate of convergence for each family.

3.1.1 Taylor-Hood-$\mathbb{P}_k$

We start by introducing a family based on Taylor-Hood [40] finite elements for velocity and pressure, and continuous or discontinuous piecewise polynomial spaces for vorticity. More precisely, for any $k \geq 1$, we consider:

$$\begin{aligned} \mathbf{V}_h &:= \{\boldsymbol{v}_h \in C(\overline{\Omega})^d : \boldsymbol{v}_h|_K \in \mathbb{P}_{k+1}(K)^d \quad \forall K \in \mathcal{T}_h\} \cap \mathrm{H}_0^1(\Omega)^d, \\ Q_h &:= \{q_h \in C(\overline{\Omega}) : q_h|_K \in \mathbb{P}_k(K) \quad \forall K \in \mathcal{T}_h\} \cap \mathrm{L}_0^2(\Omega), \\ \mathbf{W}_h^1 &:= \{\boldsymbol{\theta}_h \in C(\overline{\Omega})^{d(d-1)/2} : \boldsymbol{\theta}_h|_K \in \mathbb{P}_k(K)^{d(d-1)/2} \quad \forall K \in \mathcal{T}_h\}, \\ \mathbf{W}_h^2 &:= \{\boldsymbol{\theta}_h \in \mathrm{L}^2(\Omega)^{d(d-1)/2} : \boldsymbol{\theta}_h|_K \in \mathbb{P}_k(K)^{d(d-1)/2} \quad \forall K \in \mathcal{T}_h\}. \end{aligned} \tag{3.4}$$

It is well known that $(\mathbf{V}_h, Q_h)$ satisfies the inf-sup condition (3.1) (see [17],[18],[39]). In addition, we will consider, for the vorticity approximation, continuous ($\mathbf{W}_h^1$) and discontinuous ($\mathbf{W}_h^2$) polynomial spaces.

Now, we recall the approximation properties of the finite element subspaces introduced in (3.4).

Assume that $\boldsymbol{u} \in \mathrm{H}^{1+s}(\Omega)^d$, $p \in \mathrm{H}^s(\Omega)$ and $\boldsymbol{\omega} \in \mathrm{H}^s(\Omega)^{d(d-1)/2}$, for some $s \in (1/2, k+1]$. Then there exists $C > 0$, independent of h, such that

$$\inf_{\boldsymbol{v}_h \in \mathbf{V}_h} \|\boldsymbol{u} - \boldsymbol{v}_h\|_{1,\Omega} \leq Ch^s \|\boldsymbol{u}\|_{\mathrm{H}^{1+s}(\Omega)^d}, \tag{3.5a}$$

$$\inf_{q_h \in Q_h} \|p - q_h\|_{0,\Omega} \leq Ch^s \|p\|_{\mathrm{H}^s(\Omega)}, \tag{3.5b}$$

$$\inf_{\boldsymbol{\theta}_h \in \mathbf{W}_h^1} \|\boldsymbol{\omega} - \boldsymbol{\theta}_h\|_{0,\Omega} \leq Ch^s \|\boldsymbol{\omega}\|_{\mathrm{H}^s(\Omega)^{d(d-1)/2}}, \tag{3.5c}$$

$$\inf_{\boldsymbol{\theta}_h \in \mathbf{W}_h^2} \|\boldsymbol{\omega} - \boldsymbol{\theta}_h\|_{0,\Omega} \leq Ch^s \|\boldsymbol{\omega}\|_{\mathrm{H}^s(\Omega)^{d(d-1)/2}}. \tag{3.5d}$$

The following theorem provides the rate of convergence of our augmented mixed finite element scheme (3.2).

Theorem 3.2 *Let $k \geq 1$ be an integer, and let $\mathbf{V}_h, Q_h$ and W_h^i, $i = 1, 2$ be given by (3.4). Let $(\boldsymbol{u}, \boldsymbol{\omega}, p) \in \mathrm{H}_0^1(\Omega)^d \times \mathrm{L}^2(\Omega)^{d(d-1)/2} \times \mathrm{L}_0^2(\Omega)$ and $(\boldsymbol{u}_h, \boldsymbol{\omega}_h, p_h) \in \mathbf{V}_h \times \mathbf{W}_h^i \times Q_h$ be the unique solutions to the continuous and discrete problems (2.7) and (3.2), respectively. Assume that $\boldsymbol{u} \in \mathrm{H}^{1+s}(\Omega)^d$, $\boldsymbol{\omega} \in \mathrm{H}^s(\Omega)^{d(d-1)/2}$ and $p \in \mathrm{H}^s(\Omega)$, for some $s \in (1/2, k+1]$. Then, there exists $\hat{C} > 0$, independent of h, such that*

$$\|(\boldsymbol{u}, \boldsymbol{\omega}) - (\boldsymbol{u}_h, \boldsymbol{\omega}_h)\| + \|p - p_h\|_{0,\Omega} \leq \hat{C} h^s (\|\boldsymbol{u}\|_{\mathrm{H}^{1+s}(\Omega)^d} + \|\boldsymbol{\omega}\|_{\mathrm{H}^s(\Omega)^{d(d-1)/2}} + \|p\|_{\mathrm{H}^s(\Omega)}).$$

Proof The proof follows from (3.3b) and the approximation properties given in (3.5a)-(3.5d). □

3.1.2 MINI-element-$\mathbb{P}_k$

The second family of finite element is based on the so-called MINI-element for velocity and pressure, and continuous or discontinuous piecewise polynomials for vorticity.

Let us introduce the following spaces (see [19, Sections 8.6 and 8.7], for further details):

$$\begin{aligned}
\mathbf{U}_h &:= \{\boldsymbol{v}_h \in C(\overline{\Omega})^d : \boldsymbol{v}_h|_K \in \mathbb{P}_k(K)^d \quad \forall K \in \mathcal{T}_h\}, \\
\mathbb{B}(b_K \nabla H_h) &:= \{\boldsymbol{v}_{hb} \in \mathrm{H}^1(\Omega)^d : \boldsymbol{v}_{hb}|_K = b_K \nabla(q_h)|_K \text{ for some } q_h \in H_h\},
\end{aligned}$$

where b_K is the standard (cubic or quartic) bubble function $\lambda_1 \cdots \lambda_{d+1} \in \mathbb{P}_{d+1}(K)$, and let us define the following finite element subspaces:

$$\begin{aligned}
Q_h &:= \{q_h \in C(\overline{\Omega}) : q_h|_K \in \mathbb{P}_k(K) \quad \forall K \in \mathcal{T}_h\} \cap \mathrm{L}_0^2(\Omega), \\
\mathbf{V}_h &:= \mathbf{U}_h \oplus \mathbb{B}(b_K \nabla Q_h) \cap \mathrm{H}_0^1(\Omega)^d, \\
\mathbf{W}_h^1 &:= \{\boldsymbol{\theta}_h \in C(\overline{\Omega})^{d(d-1)/2} : \boldsymbol{\theta}_h|_K \in \mathbb{P}_k(K)^{d(d-1)/2} \quad \forall K \in \mathcal{T}_h\}, \\
\mathbf{W}_h^2 &:= \{\boldsymbol{\theta}_h \in \mathrm{L}^2(\Omega)^{d(d-1)/2} : \boldsymbol{\theta}_h|_K \in \mathbb{P}_k(K)^{d(d-1)/2} \quad \forall K \in \mathcal{T}_h\}.
\end{aligned} \tag{3.6}$$

The rate of convergence of our augmented mixed finite element scheme considering the above discrete spaces (3.6) is as follows.

Theorem 3.3 *Let $k \geq 1$ be an integer, and let $\mathbf{V}_h, Q_h$ and W_h^i, $i = 1, 2$ be given by (3.6). Let $(\boldsymbol{u}, \boldsymbol{\omega}, p) \in \mathrm{H}_0^1(\Omega)^d \times \mathrm{L}^2(\Omega)^{d(d-1)/2} \times \mathrm{L}_0^2(\Omega)$ and $(\boldsymbol{u}_h, \boldsymbol{\omega}_h, p_h) \in \mathbf{V}_h \times \mathbf{W}_h^i \times Q_h$ be the unique solutions to the continuous and discrete problems (2.7) and (3.2), respectively. Assume that $\boldsymbol{u} \in \mathrm{H}^{1+s}(\Omega)^d$, $\boldsymbol{\omega} \in \mathrm{H}^s(\Omega)^{d(d-1)/2}$ and $p \in \mathrm{H}^s(\Omega)$, for some $s \in (1/2, k]$. Then, there exists $\hat{C} > 0$, independent of h, such that*

$$\|(\boldsymbol{u}, \boldsymbol{\omega}) - (\boldsymbol{u}_h, \boldsymbol{\omega}_h)\| + \|p - p_h\|_{0,\Omega} \leq \hat{C} h^s (\|\boldsymbol{u}\|_{\mathrm{H}^{1+s}(\Omega)^d} + \|\boldsymbol{\omega}\|_{\mathrm{H}^s(\Omega)^{d(d-1)/2}} + \|p\|_{\mathrm{H}^s(\Omega)}).$$

Remark 3.1 The unique solvability of the discrete problem (3.2) given by Theorem 3.1, follows similarly to the continuous case, by using the Babuška-Brezzi theory. In fact, the ellipticity is obtained exactly as in the proof of Lemma 2.2, whereas the inf-sup condition (3.1) is guaranteed thanks to the choice of the families of finite element given by (3.4) or (3.6).

4 A posteriori error estimator

In this section, we propose a residual-based a posteriori error estimator. Moreover, we prove its reliability and efficiency. For simplicity, we will restrict ourselves to the two-dimensional case. In addition, we will consider families of finite elements with continuous pressure and vorticity.

We start by introducing some notation to be used through this section. For each $T \in \mathcal{T}_h$ we let $\mathcal{E}(T)$ be the set of edges of T, and we denote by $\mathcal{E}_h$ the set of all edges in $\mathcal{T}_h$, that is

$$\mathcal{E}_h = \mathcal{E}_h(\Omega) \cup \mathcal{E}_h(\Gamma),$$

where $\mathcal{E}_h(\Omega) := \{e \in \mathcal{E}_h : e \subset \Omega\}$, and $\mathcal{E}_h(\Gamma) := \{e \in \mathcal{E}_h : e \subset \Gamma\}$. In what follows, h_e stands for the diameter of a given edge $e \in \mathcal{E}_h$, $\boldsymbol{t}_e = (-n_2, n_1)$, where $\boldsymbol{n}_e = (n_1, n_2)$ is a fix unit normal vector of e. Now, let $q \in \mathrm{L}^2(\Omega)$ such that $q|_T \in C(T)$ for each $T \in \mathcal{T}_h$, then given $e \in \mathcal{E}_h(\Omega)$, we denote by $[q]$ the jump of q across e, that is $[q] := (q|_{T'})|_e - (q|_{T''})|_e$, where T' and T'' are the triangles of $\mathcal{T}_h$ sharing the edge e. Moreover, let $\boldsymbol{v} \in \mathrm{L}^2(\Omega)^2$ such that $\boldsymbol{v}|_T \in C(T)^2$ for each $T \in \mathcal{T}_h$. Then, given $e \in \mathcal{E}_h(\Omega)$, we denote by $[\boldsymbol{v} \cdot \boldsymbol{t}]$ the tangential jump of $\boldsymbol{v}$ across e, that is, $[\boldsymbol{v} \cdot \boldsymbol{t}] := ((\boldsymbol{v}|_{T'})|_e - (\boldsymbol{v}|_{T''})|_e) \cdot \boldsymbol{t}_e$, where T' and T'' are the triangles of $\mathcal{T}_h$ sharing the edge e.

Next, let $k \geq 1$ be an integer, and let $\mathbf{V}_h, Q_h$ and $\mathbf{W}_h^1$ be given as in (3.4) or (3.6). Let $(\boldsymbol{u}, \omega, p) \in \mathrm{H}_0^1(\Omega)^2 \times \mathrm{L}^2(\Omega) \times \mathrm{L}_0^2(\Omega)$ and $(\boldsymbol{u}_h, \omega_h, p_h) \in \mathbf{V}_h \times \mathbf{W}_h^1 \times Q_h$ be the unique solutions to the continuous and discrete problems (2.7) and (3.2), respectively. We introduce for each $T \in \mathcal{T}_h$ the local *a posteriori* error indicator as

$$\Theta_T^2 := h_T^2 \|\boldsymbol{f} - \sigma \boldsymbol{u}_h - \nu \,\mathbf{curl}\, \omega_h - (\boldsymbol{\beta} \cdot \nabla)\boldsymbol{u}_h + 2\boldsymbol{\varepsilon}(\boldsymbol{u}_h)\nabla\nu - \nabla p_h\|_{0,T}^2 + \|\omega_h - \mathrm{rot}\, \boldsymbol{u}_h\|_{0,T}^2 + \|\,\mathrm{div}\; \boldsymbol{u}_h\|_{0,T}^2,$$

and define its global counterpart as

$$\Theta := \left\{ \sum_{T \in \mathcal{T}_h} \Theta_T^2 \right\}^{1/2}. \tag{4.1}$$

Let us now establish reliability and efficiency of (4.1).

4.1 Reliability

We begin by recalling that the continuous dependence result given in Theorem 2.1 is equivalent to the global inf–sup condition for the continuous formulation (2.7). Then, applying this estimate to the error $(\boldsymbol{u} - \boldsymbol{u}_h, \omega - \omega_h, p - p_h)$, we obtain

$$\|(\boldsymbol{u}, \omega) - (\boldsymbol{u}_h, \omega_h)\| + \|p - p_h\|_{0,\Omega} \leq C_{glob} \sup_{(\boldsymbol{v}_h, \theta_h, q_h) \in} \frac{\mathcal{R}(\boldsymbol{v}, \theta, q)}{\|(\boldsymbol{v}, \theta, q)\|}, \tag{4.2}$$

where the residual functional $\mathcal{R}$ is defined by

$$\mathcal{R}(\boldsymbol{v}, \theta, q) = A((\boldsymbol{u} - \boldsymbol{u}_h, \omega - \omega_h), (\boldsymbol{v}, \theta)) + B((\boldsymbol{v}, \theta), p - p_h) + B((\boldsymbol{u} - \boldsymbol{u}_h, \omega - \omega_h), q), \tag{4.3}$$

for all $(\boldsymbol{v}, \theta, q) \in \mathrm{H}_0^1(\Omega)^2 \times \mathrm{L}^2(\Omega) \times \mathrm{L}_0^2(\Omega)$.

Some technical results are provided beforehand. Let us first recall the Clément-type interpolation operator $\mathcal{I}_h : \mathrm{H}^1_0(\Omega) \to Y_h$, where $Y_h := \{v_h \in C(\overline{\Omega}) \cap \mathrm{H}^1_0(\Omega) : v_h\big|_T \in \mathbb{P}_1(T), \forall T \in \mathcal{T}_h\}$. This operator satisfies the following local approximation properties (cf. [26]).

Lemma 4.1 *There exist positive constants C_1 and C_2 such that for all $v \in \mathrm{H}^1(\Omega)$ there hold*

$$\|v - \mathcal{I}_h v\|_{0,T} \le C_1 h_T |v|_{1,w_T} \quad \forall T \in \mathcal{T}_h, \tag{4.4a}$$

$$\|v - \mathcal{I}_h v\|_{0,e} \le C_2 h_e^{1/2} |v|_{1,w_e} \quad \forall e \in \mathcal{E}_h(\Omega), \tag{4.4b}$$

where $w_T := \bigcup\{T' \in \mathcal{T}_h : T' \cap T \neq \emptyset\}$ and $w_e := \bigcup\{T' \in \mathcal{T}_h : T' \cap e \neq \emptyset\}$

The main result of this section is stated as follows.

Theorem 4.1 *There exists a positive constant C_{rel}, independent of the discretisation parameter h, such that*

$$\|(\boldsymbol{u}, \omega) - (\boldsymbol{u}_h, \omega_h)\| + \|p - p_h\|_{0,\Omega} \le C_{\mathrm{rel}}\, \Theta. \tag{4.5}$$

Proof From (4.3) and the continuous problem (2.7), we have that,

$$\begin{aligned}
\mathcal{R}(\boldsymbol{v}, \theta, q) &= \int_\Omega \boldsymbol{f} \cdot \boldsymbol{v} - \Big(A((\boldsymbol{u}_h, \omega_h), (\boldsymbol{v}, \theta)) + B((\boldsymbol{v}, \theta), p_h) + B((\boldsymbol{u}_h, \omega_h), q)\Big)\\
&= \int_\Omega (\boldsymbol{f} - \sigma \boldsymbol{u}_h - (\boldsymbol{\beta} \cdot \nabla)\boldsymbol{u}_h + 2\boldsymbol{\varepsilon}(\boldsymbol{u}_h)\nabla\nu) \cdot \boldsymbol{v} - \int_\Omega \nu(\omega_h - \operatorname{rot} \boldsymbol{u}_h)\theta\\
&- \kappa_1 \int_\Omega (\operatorname{rot} \boldsymbol{u}_h - \omega_h) \operatorname{rot} \boldsymbol{v} - \kappa_2 \int_\Omega \operatorname{div} \boldsymbol{u}_h \operatorname{div} \boldsymbol{v}\\
&- \left(\int_\Omega \nu\omega_h \operatorname{rot} \boldsymbol{v} + \int_\Omega \omega_h(\nabla\nu \times \boldsymbol{v})\right) + \int_\Omega p_h \operatorname{div} \boldsymbol{v} + \int_\Omega q \operatorname{div} \boldsymbol{u}_h.
\end{aligned}$$

Using the identity $\operatorname{rot}(\nu\boldsymbol{v}) = \nabla\nu \times \boldsymbol{v} + \nu \operatorname{rot} \boldsymbol{v}$ and integration by parts on the above residual (cf. (1.2)), we obtain

$$\begin{aligned}
\mathcal{R}(\boldsymbol{v}, \theta, q) = &\int_\Omega (\boldsymbol{f} - \sigma \boldsymbol{u}_h - (\boldsymbol{\beta} \cdot \nabla)\boldsymbol{u}_h + 2\boldsymbol{\varepsilon}(\boldsymbol{u}_h)\nabla\nu) \cdot \boldsymbol{v} - \int_\Omega \nu(\omega_h - \operatorname{rot} \boldsymbol{u}_h)\theta\\
&- \kappa_1 \int_\Omega (\operatorname{rot} \boldsymbol{u}_h - \omega_h) \operatorname{rot} \boldsymbol{v} - \kappa_2 \int_\Omega \operatorname{div} \boldsymbol{u}_h \operatorname{div} \boldsymbol{v} + \int_\Omega q \operatorname{div} \boldsymbol{u}_h\\
&- \sum_{T \in \mathcal{T}_h} \left(\int_T \nu\, \mathbf{curl}\, \omega_h \cdot \boldsymbol{v} - \langle \boldsymbol{v} \cdot \boldsymbol{t}, \nu\omega_h\rangle_{\partial T} - \int_T \nabla p_h \cdot \boldsymbol{v} + \langle \boldsymbol{v} \cdot \boldsymbol{n}, p_h\rangle_{\partial T}\right)\\
&= \sum_{T \in \mathcal{T}_h} \int_T (\boldsymbol{f} - \sigma \boldsymbol{u}_h - \nu\, \mathbf{curl}\, \omega_h - (\boldsymbol{\beta} \cdot \nabla)\boldsymbol{u}_h + 2\boldsymbol{\varepsilon}(\boldsymbol{u}_h)\nabla\nu - \nabla p_h) \cdot \boldsymbol{v}\\
&- \int_\Omega \nu(\omega_h - \operatorname{rot} \boldsymbol{u}_h)\theta - \kappa_1 \int_\Omega (\operatorname{rot} \boldsymbol{u}_h - \omega_h) \operatorname{rot} \boldsymbol{v} - \kappa_2 \int_\Omega \operatorname{div} \boldsymbol{u}_h \operatorname{div} \boldsymbol{v} + \int_\Omega q \operatorname{div} \boldsymbol{u}_h,
\end{aligned}$$

where we have used the fact that ω_h and p_h are piecewise continuous functions.

Hence, since $\mathcal{R}(\boldsymbol{v}_h, \theta_h, q_h) = 0$, which follows from (4.3), we obtain

$$\begin{aligned}
\mathcal{R}(\boldsymbol{v}, \theta, q) &= \mathcal{R}(\boldsymbol{v} - \boldsymbol{v}_h, \theta - \theta_h, q - q_h)\\
&= \sum_{T \in \mathcal{T}_h} \int_T \big(\boldsymbol{f} - \sigma \boldsymbol{u}_h - \nu\, \mathbf{curl}\, \omega_h - (\boldsymbol{\beta} \cdot \nabla)\boldsymbol{u}_h + 2\boldsymbol{\varepsilon}(\boldsymbol{u}_h)\nabla\nu - \nabla p_h\big) \cdot (\boldsymbol{v} - \boldsymbol{v}_h)
\end{aligned}$$

$$- \int_\Omega \nu(\omega_h - \operatorname{rot} \boldsymbol{u}_h)(\theta - \theta_h) - \kappa_1 \int_\Omega (\operatorname{rot} \boldsymbol{u}_h - \omega_h) \operatorname{rot}(\boldsymbol{v} - \boldsymbol{v}_h)$$
$$- \kappa_2 \int_\Omega \operatorname{div} \boldsymbol{u}_h \operatorname{div}(\boldsymbol{v} - \boldsymbol{v}_h) + \int_\Omega (q - q_h) \operatorname{div} \boldsymbol{u}_h.$$

Thus, it suffices to take $\boldsymbol{v}_h := \mathcal{I}_h(\boldsymbol{v})$ (cf. Lemma 4.1), and $\theta_h := \Pi(\theta)$ and $q_h := \Pi(q)$ with Π being the L^2 projection onto the piecewise constant functions. And then, using the Cauchy-Schwarz inequality, triangle inequality, properties for $\mathcal{I}_h$ given by Lemma 4.1 and [32, Lemma 1.127], and approximation properties for Π, we obtain

$$\begin{aligned}
\mathcal{R}(\boldsymbol{v}, \theta, q) &\leq C_1 \sum_{T \in \mathcal{T}_h} h_T \|\boldsymbol{f} - \sigma \boldsymbol{u}_h - \nu \,\mathbf{curl}\, \omega_h - (\boldsymbol{\beta} \cdot \nabla)\boldsymbol{u}_h + 2\boldsymbol{\varepsilon}(\boldsymbol{u}_h)\nabla\nu - \nabla p_h\|_{0,T} |\boldsymbol{v}|_{1,w_T} \\
&+ \sum_{T \in \mathcal{T}_h} (\nu_1 + \kappa_1) \|\omega_h - \operatorname{rot} \boldsymbol{u}_h\|_{0,T} (C_3 \|\theta\|_{0,T} + |\boldsymbol{v} - \boldsymbol{v}_h|_{1,T}) \\
&+ \sum_{T \in \mathcal{T}_h} (\kappa_2 + 1) \|\operatorname{div} \boldsymbol{u}_h\|_{0,T} (|\boldsymbol{v} - \boldsymbol{v}_h|_{1,T} + C_4 \|q\|_{0,T}) \\
&\leq \widehat{C}_1 \left(\sum_{T \in \mathcal{T}_h} h_T^2 \|f - \sigma \boldsymbol{u}_h - \nu \,\mathbf{curl}\, \omega_h - (\boldsymbol{\beta} \cdot \nabla)\boldsymbol{u}_h + 2\boldsymbol{\varepsilon}(\boldsymbol{u}_h)\nabla\nu - \nabla p_h\|_{0,T}^2 \right)^{1/2} \|\boldsymbol{v}\|_{1,\Omega} \\
&+ \widehat{C}_2 \left(\sum_{T \in \mathcal{T}_h} \|\omega_h - \operatorname{rot} \boldsymbol{u}_h\|_{0,T}^2 \right)^{1/2} (\|\theta\|_{0,\Omega} + \|\boldsymbol{v}\|_{1,\Omega}) \\
&+ \widehat{C}_3 \left(\sum_{T \in \mathcal{T}_h} \|\operatorname{div} \boldsymbol{u}_h\|_{0,T}^2 \right)^{1/2} (\|\boldsymbol{v}\|_{1,\Omega} + \|q\|_{0,\Omega}).
\end{aligned}$$

Therefore, the proof follows from (4.2) and the above estimate.

□

4.2 Efficiency

This subsection deals with the efficiency of the *a posteriori* error estimator. For simplicity, we will assume that the given convective velocity $\boldsymbol{\beta}$ and the viscosity ν are polynomial functions both of degree s. The general case can be proved by repeating the same arguments and requiring an additional regularity for the data.

A major role in the proof of efficiency is played by element and edge bubbles (locally supported non-negative functions), whose definition we recall in what follows. For $T \in \mathcal{T}_h(\Omega)$ and $e \in \mathcal{E}(T)$, let ψ_T and ψ_e, respectively, be the interior and edge bubble functions defined as in, e.g., [1]. Let $\psi_T \in \mathbb{P}_3(T)$ with $supp(\psi_T) \subset T$, $\psi_T = 0$ on ∂T and $0 \leq \psi_T \leq 1$ in T. Moreover, let $\psi_e|_T \in \mathbb{P}_2(T)$ with $supp(\psi_e) \subset \Omega_e := \{T' \in \mathcal{T}_h(\Omega) : e \in \mathcal{E}(T')\}$, $\psi_e = 0$ on $\partial T \setminus e$, and $0 \leq \psi_e \leq 1$ in Ω_e. Again, let us recall an extension operator $E : C^0(e) \mapsto C^0(T)$ that satisfies $E(q) \in \mathbb{P}_k(T)$ and $E(q)|_e = q$ for all $q \in \mathbb{P}_k(e)$ and for all $k \in \mathbb{N} \cup \{0\}$.

We now summarise the properties of ψ_T, ψ_e and E in the following lemma (see [1,53]).

Lemma 4.2 *The following properties hold:*

(i) For $T \in \mathcal{T}_h$ and for $v \in \mathbb{P}_k(T)$, there is a positive constant C_1 such that

$$C_1^{-1} \|v\|_{0,T}^2 \leq \int_T \psi_T v^2 \, dx \leq C_1 \|v\|_{0,T}^2,$$

$$C_1^{-1}\, \|v\|_{0,T}^2 \le \|\psi v\|_{0,T}^2 + h_T^2 |\psi v|_{1,T}^2 \le C_1 \|v\|_{0,T}^2.$$

(ii) For $e \in \mathcal{E}_h$ and $v \in \mathbb{P}_k(e)$, there exists a positive constant, say C_1, such that

$$C_1^{-1}\, \|v\|_{0,e}^2 \le \int_e \psi_e v^2 ds \le C_1 \|v\|_{0,e}^2.$$

(iii) For $T \in \mathcal{T}_h$ with $e \in \mathcal{E}(T)$ and for all $v \in \mathbb{P}_k(e)$, there is a positive constant, again say C_1, such that

$$\|\psi_e^{1/2}\, E(v)\|_{0,T}^2 \le C_1 h_e\, \|v\|_{0,e}^2.$$

The following classical result which states an inverse estimate will also be used.

Lemma 4.3 *Let $k, l, m \in \mathbb{N} \cup \{0\}$ such that $l \le m$. Then, there exists $\tilde{C} > 0$, depending only on k, l, m and the shape regularity of the triangulations, such that for each triangle T there holds*

$$|q|_{m,T} \le \tilde{C} h_T^{l-m} |q|_{l,T} \quad \forall q \in \mathbb{P}_k(T).$$

In order to prove the efficiency of the a posteriori error estimator, we will bound each term defining Θ_T in terms of local errors.

Theorem 4.2 *There is a positive constant C_{eff}, independent of h, such that*

$$C_{\mathrm{eff}}\, \Theta \le \ \|(\boldsymbol{u}, \omega) - (\boldsymbol{u}_h, \omega_h)\| + \|p - p_h\|_{0,\Omega} + \text{h.o.t.},$$

where h.o.t. *denotes higher-order terms.*

Proof Using that $\omega - \operatorname{rot} \boldsymbol{u} = 0$ and $\operatorname{div} \boldsymbol{u} = 0$ in Ω (see (2.3b) and (2.3c), respectively), we immediately have that

$$\|\omega_h - \operatorname{rot} \boldsymbol{u}_h\|_{0,T} + \|\operatorname{div} \boldsymbol{u}_h\|_{0,T} \le \|\operatorname{rot}(\boldsymbol{u} - \boldsymbol{u}_h)\|_{0,T} + \|\operatorname{div}(\boldsymbol{u} - \boldsymbol{u}_h)\|_{0,T} + \|\omega - \omega_h\|_{0,T}.$$

On the other hand, with the help of the $\mathrm{L}^2(T)^2$-orthogonal projection $\mathcal{P}_T^\ell$ onto $\mathbb{P}_\ell(T)^2$, for $\ell \ge (s + k + 1)$, with respect to the weighted L^2-inner product $(\psi_T \boldsymbol{f}, \boldsymbol{g})_{0,T}$, for $\boldsymbol{f}, \boldsymbol{g} \in \mathrm{L}^2(T)^2$, it now follows that

$$\begin{aligned}
&\|\boldsymbol{f} - \sigma \boldsymbol{u}_h - \nu \,\mathbf{curl}\, \omega_h - (\boldsymbol{\beta} \cdot \nabla) \boldsymbol{u}_h + 2\boldsymbol{\varepsilon}(\boldsymbol{u}_h) \nabla \nu - \nabla p_h\|_{0,T}^2 \\
&\qquad = \|\boldsymbol{f} - \mathcal{P}_T^\ell(\boldsymbol{f}) + \mathcal{P}_T^\ell(\boldsymbol{f}) - \sigma \boldsymbol{u}_h - \nu \,\mathbf{curl}\, \omega_h - (\boldsymbol{\beta} \cdot \nabla) \boldsymbol{u}_h + 2\boldsymbol{\varepsilon}(\boldsymbol{u}_h) \nabla \nu - \nabla p_h\|_{0,T}^2 \\
&\qquad \le \|\boldsymbol{f} - \mathcal{P}_T^\ell(\boldsymbol{f})\|_{0,T}^2 + \|\mathcal{P}_T^\ell(\boldsymbol{f}) - \sigma \boldsymbol{u}_h - \nu \,\mathbf{curl}\, \omega_h - (\boldsymbol{\beta} \cdot \nabla) \boldsymbol{u}_h + 2\boldsymbol{\varepsilon}(\boldsymbol{u}_h) \nabla \nu - \nabla p_h\|_{0,T}^2 \\
&\qquad = \|\boldsymbol{f} - \mathcal{P}_T^\ell(\boldsymbol{f})\|_{0,T}^2 + \|\mathcal{P}_T^\ell(\boldsymbol{f} - \sigma \boldsymbol{u}_h - \nu \,\mathbf{curl}\, \omega_h - (\boldsymbol{\beta} \cdot \nabla) \boldsymbol{u}_h + 2\boldsymbol{\varepsilon}(\boldsymbol{u}_h) \nabla \nu - \nabla p_h)\|_{0,T}^2.
\end{aligned}$$

For the second term on the right-hand side, an application of Lemma 4.2 shows that

$$\begin{aligned}
&\|\mathcal{P}_T^\ell(\boldsymbol{f} - \sigma \boldsymbol{u}_h - \nu \,\mathbf{curl}\, \omega_h - (\boldsymbol{\beta} \cdot \nabla) \boldsymbol{u}_h + 2\boldsymbol{\varepsilon}(\boldsymbol{u}_h) \nabla \nu - \nabla p_h)\|_{0,T}^2 \\
&\qquad \le \|\psi_T^{1/2} \mathcal{P}_T^\ell(\boldsymbol{f} - \sigma \boldsymbol{u}_h - \nu \,\mathbf{curl}\, \omega_h - (\boldsymbol{\beta} \cdot \nabla) \boldsymbol{u}_h + 2\boldsymbol{\varepsilon}(\boldsymbol{u}_h) \nabla \nu - \nabla p_h)\|_{0,T}^2 \\
&\qquad = \int_T \psi_T \mathcal{P}_T^\ell(\boldsymbol{f} - \sigma \boldsymbol{u}_h - \nu \,\mathbf{curl}\, \omega_h - (\boldsymbol{\beta} \cdot \nabla) \boldsymbol{u}_h + 2\boldsymbol{\varepsilon}(\boldsymbol{u}_h) \nabla \nu - \nabla p_h) \\
&\qquad\qquad \times (\boldsymbol{f} - \sigma \boldsymbol{u}_h - \nu \,\mathbf{curl}\, \omega_h - (\boldsymbol{\beta} \cdot \nabla) \boldsymbol{u}_h + 2\boldsymbol{\varepsilon}(\boldsymbol{u}_h) \nabla \nu - \nabla p_h),
\end{aligned}$$

where we have used the fact that $\mathcal{P}_T^\ell$ is the $L^2(T)^2$-orthogonal projection. Thus, from the above inequality, and (2.3a) (cf. Remark 2.4), we can deduce that

$$\|\mathcal{P}_T^\ell(\boldsymbol{f} - \sigma \boldsymbol{u}_h - \nu \,\mathbf{curl}\, \omega_h - (\boldsymbol{\beta} \cdot \nabla) \boldsymbol{u}_h + 2\boldsymbol{\varepsilon}(\boldsymbol{u}_h) \nabla \nu - \nabla p_h)\|_{0,T}^2$$

$$\leq \int_T \psi_T \mathcal{P}_T^\ell(\boldsymbol{f} - \sigma \boldsymbol{u}_h - \nu\,\mathbf{curl}\,\omega_h - (\boldsymbol{\beta}\cdot\nabla)\boldsymbol{u}_h + 2\boldsymbol{\varepsilon}(\boldsymbol{u}_h)\nabla\nu - \nabla p_h)$$
$$\times\,(\sigma(\boldsymbol{u}-\boldsymbol{u}_h) + \nu\,\mathbf{curl}(\omega-\omega_h) + (\boldsymbol{\beta}\cdot\nabla)(\boldsymbol{u}-\boldsymbol{u}_h) - 2\boldsymbol{\varepsilon}(\boldsymbol{u}-\boldsymbol{u}_h)\nabla\nu + \nabla(p-p_h)).$$

Next, using that the viscosity is a polynomial function, the bound follows by integration by parts of the terms $\mathbf{curl}(\omega-\omega_h)$ and $\nabla(p-p_h)$, Cauchy-Schwarz inequality and an inverse inequality (cf. Lemma 4.3).

We end the proof by observing that the required efficiency of the a posteriori error estimator follows straightforwardly from the previous bounds and assuming an additional regularity for source term $\boldsymbol{f}$. □

5 Numerical results

In this section, we present some numerical experiments carried out with the finite element method proposed and analysed in Section 3. We also present two numerical examples in $\mathbb{R}^2$, confirming the reliability and efficiency of the a posteriori error estimator Θ derived in Section 4, and showing the behaviour of the associated adaptive algorithm. The solution of all linear systems is carried out with the multifrontal massively parallel sparse direct solver MUMPS.

Individual errors are denoted by

$$e(\boldsymbol{u}) = \|\boldsymbol{u}-\boldsymbol{u}_h\|_{1,\Omega}, \quad e(\boldsymbol{\omega}) = \|\boldsymbol{\omega}-\boldsymbol{\omega}_h\|_{0,\Omega}, \quad e(p) = \|p-p_h\|_{0,\Omega}.$$

We proceed to construct a series of uniformly successively refined triangular meshes for Ω and compute convergence rates as follows

$$r(\boldsymbol{u}) = \frac{\log(e(\boldsymbol{u})/\widehat{e}(\boldsymbol{u}))}{\log(h/\hat{h})}, \qquad r(\boldsymbol{\omega}) = \frac{\log(e(\boldsymbol{\omega})/\widehat{e}(\boldsymbol{\omega}))}{\log(h/\hat{h})}, \qquad r(p) = \frac{\log(e(p)/\widehat{e}(p))}{\log(h/\hat{h})}, \tag{5.1}$$

where $e, \widehat{e}$ denote errors computed on two consecutive meshes of sizes $h, \hat{h}$, respectively.

5.1 Example 1: Convergence test using manufactured solutions

The first test consists of approximating closed-form solutions on a two-dimensional domain $\Omega = (0,1)^2$. We construct the forcing term $\boldsymbol{f}$ so that the exact solution to (2.3a)-(2.3c) is given by the following smooth functions

$$p(x,y) := \left(\left(x-\frac{1}{2}\right)^3 y^2 + (1-x)^3\left(y-\frac{1}{2}\right)^3\right),$$
$$\boldsymbol{u}(x,y) := \mathbf{curl}(1000x^2(1-x)^4y^3(1-y)^2), \qquad \omega(x,y) := \operatorname{rot}\boldsymbol{u}(x,y),$$

which satisfy the incompressibility constraint as well as the boundary conditions. In addition, we take

$$\boldsymbol{\beta}(x,y) := \boldsymbol{u}(x,y),$$

and two specifications for the variable viscosity are considered,

$$\nu_a(x,y) = \nu_0 + (\nu_1-\nu_0)xy, \qquad \nu_b(x,y) = \nu_0 + (\nu_1-\nu_0)exp(-10^{13}((x-0.5)^{10} + (y-0.5)^{10})).$$

We use $\nu_0 = 0.001$, $\nu_1 = 1$, $\kappa_1 = \frac{2}{3}\nu_0$, $\kappa_2 = \frac{\nu_0}{2}$ and $\sigma = 100$.

The error history of the method introduced in Section 3.1.1 with discontinuous finite elements for vorticity ($\mathbf{W}_h^2$) for $k=1$ and for the two different viscosity functions is collected in Tables 5.1 and 5.2, respectively. These values indicate optimal accuracy $O(h^2)$ for $k=1$, and for ν_a and ν_b, according to Theorem 3.2.

h	$\|\boldsymbol{u}-\boldsymbol{u}_h\|_{1,\Omega}$	$r(\boldsymbol{u})$	$\|\omega-\omega_h\|_{0,\Omega}$	$r(\omega)$	$\|p-p_h\|_{0,\Omega}$	$r(p)$
0.7071	10.86	–	9.1110	–	2.5470	–
0.3536	4.4240	1.3	3.5500	1.4	1.5330	0.7
0.1768	1.2540	1.8	0.9854	1.9	0.3493	2.1
0.0883	0.3492	1.8	0.2470	2.0	0.0622	2.4
0.0441	0.1096	1.7	0.0613	2.0	0.0107	2.5
0.0221	0.0327	1.8	0.0151	2.0	0.0020	2.4
0.0110	0.0075	2.1	0.0037	2.0	0.0004	2.2

Table 5.1 Example 1: convergence tests against analytical solutions on a sequence of uniformly refined triangulations of the domain Ω and the viscosity function ν_a.

h	$\|\boldsymbol{u}-\boldsymbol{u}_h\|_{1,\Omega}$	$r(\boldsymbol{u})$	$\|\omega-\omega_h\|_{0,\Omega}$	$r(\omega)$	$\|p-p_h\|_{0,\Omega}$	$r(p)$
0.7071	10.91	–	9.1340	–	2.1190	–
0.3536	4.489	1.3	3.6710	1.3	1.4580	0.5
0.1768	1.367	1.7	1.1200	1.7	0.2789	2.4
0.0883	0.366	1.9	0.2951	1.9	0.0482	2.5
0.0441	0.113	1.7	0.0864	1.8	0.0070	2.8
0.0221	0.036	1.6	0.0220	2.0	0.0014	2.3
0.0110	0.007	2.1	0.0046	2.2	0.0003	2.2

Table 5.2 Example 1: convergence tests against analytical solutions on a sequence of uniformly refined triangulations of the domain Ω and the viscosity function ν_b.

5.2 Example 2: Convergence in 3D

The aim of this numerical test is to assess the accuracy of the method in the 3D case. With this end, we consider the domain $\Omega := (0,1)^3$ and take $\boldsymbol{f}$ so that the exact solution is given by

$$p(x,y,z) := 1 - x^2 - y^2 - z^2,$$

$$\varphi(x,y,z) := \begin{pmatrix} x^2(1-x)^2y^2(1-y)^2z^2(1-z)^2 \\ x^2(1-x)^2y^2(1-y)^2z^2(1-z)^2 \\ x^2(1-x)^2y^2(1-y)^2z^2(1-z)^2 \end{pmatrix},$$

$$\boldsymbol{u}(x,y,z) := \mathbf{curl}(\varphi(x,y,z)), \qquad \boldsymbol{\omega}(x,y,z) := \mathbf{curl}\,\boldsymbol{u}(x,y,z),$$

We will consider the convective velocity and viscosity functions as follows:

$$\boldsymbol{\beta}(x,y,z) := \boldsymbol{u}(x,y,z), \qquad \nu_c(x,y,z) = \nu_0 + (\nu_1 - \nu_0)x^2y^2z^2.$$

We will take the following values for $\nu_0 = 0.1$ and $\nu_1 = 1$, and the stabilisation parameters as $\kappa_1 = \frac{2}{3}\nu_0$, $\kappa_2 = \frac{\nu_0}{2}$, $\sigma = 1000$. We observe that the hypothesis of Lemma 2.2 are satisfied. Additionally, we will employ the family of finite elements introduced in Section 3.1.2 for $k = 1$, that is, $\mathbf{V}_h$ approximating the velocity, and piecewise linear and continuous elements for vorticity and pressure fields.

In Table 5.3, we summarise the convergence history for a sequence of uniform meshes. We observe that the rate of convergence $O(h)$ predicted by Theorem 3.3 is attained for all quantities. Actually, the computation of $\boldsymbol{\omega}$ and p seem to be superconvergent.

Next, in Figure 5.1 we display the streamlines for the velocity and vorticity vectors, and the approximate pressure field.

t

h	$\|\boldsymbol{u}-\boldsymbol{u}_h\|_{1,\Omega}$	$r(\boldsymbol{u})$	$\|\boldsymbol{\omega}-\boldsymbol{\omega}_h\|_{0,\Omega}$	$r(\boldsymbol{\omega})$	$\|p-p_h\|_{0,\Omega}$	$r(p)$
0.866	0.01021	–	0.00299	–	0.04732	–
0.433	0.00858	0.3	0.00125	1.3	0.01399	1.8
0.288	0.00665	0.6	0.00067	1.5	0.00572	2.2
0.216	0.00513	0.9	0.00043	1.5	0.00290	2.4
0.173	0.00398	1.1	0.00030	1.5	0.00171	2.4
0.144	0.00313	1.3	0.00023	1.5	0.00112	2.3
0.123	0.00251	1.3	0.00018	1.5	0.00079	2.2

Table 5.3 Example 2: experimental convergence using homogeneous Dirichlet boundary conditions on a 3D domain Ω and the viscosity function ν_c.

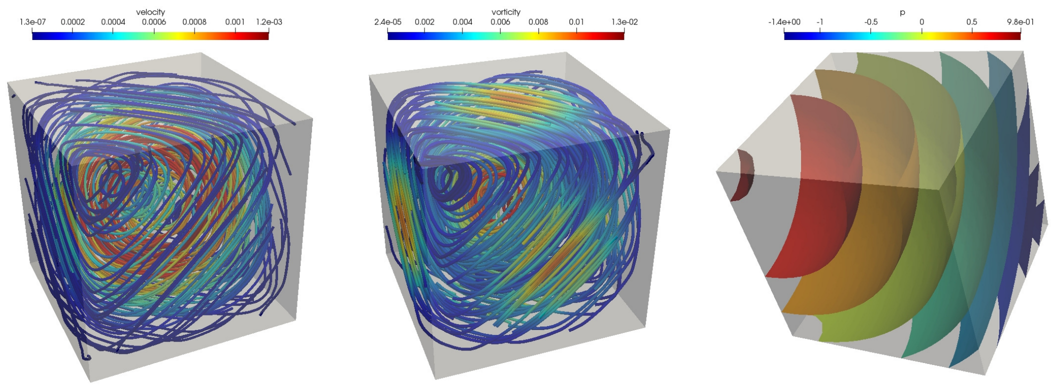

Fig. 5.1 Example 2: Approximate solutions computed using the MINI-element. Velocity streamlines (left) vorticity streamlines (centre) and pressure distribution (right).

5.3 Example 3: A posteriori error estimates and adaptive mesh refinement

In this numerical test, we test the efficiency of the a posteriori error estimator (4.1) and applying mesh refinement according to the local value of the indicator. In this case, the convergence rates are obtained by replacing the expression $\log(h/\hat{h})$ appearing in the computation of (5.1) by $-\frac{1}{2}\log(N/\hat{N})$, where N and $\hat{N}$ denote the corresponding degrees of freedom of each triangulation.

Now, we recall the definition of the so-called effectivity index as the ratio between the total error and the global error estimator, i.e.,

$$\mathtt{e}(\boldsymbol{u},\omega,p) := \left\{[e(\boldsymbol{u})]^2 + [e(\omega)]^2 + [e(p)]^2\right\}^{1/2}, \qquad \mathtt{eff}(\Theta) := \frac{\mathtt{e}(\boldsymbol{u},\omega,p)}{\Theta}.$$

We will employ the family of finite elements introduced in Section 3.1.1 for $k=1$, namely piecewise quadratic and continuous elements for velocity and piecewise linear and continuous elements for vorticity and pressure fields.

The computational domain is the nonconvex L-shaped domain $\Omega = (-1,1)^2 \setminus (0,1)^2$, where problem (2.3a)-(2.3c) admits the following exact solution

$$p(x,y) := \frac{1-x^2-y^2}{(x-0.025)^2+(y-0.025)^2} - 12.742942014/3,$$

$$\varphi(x,y) = x^2(1-x)^2y^2(1-y)^2\exp(-50((x-0.025)^2+(y-0.025)^2)),$$

$$\boldsymbol{u}(x,y) := \mathbf{curl}(\varphi(x,y)), \qquad \omega(x,y) := \operatorname{rot}\boldsymbol{u}(x,y),$$

which satisfy the incompressibility constraint as well as the boundary conditions. We will consider the convective velocity and viscosity functions as follows:

$$\boldsymbol{\beta}(x,y) := \boldsymbol{u}(x,y),$$

$$\nu_d(x,y) = \nu_0 + \frac{721}{16}(\nu_1 - \nu_0)x^2(1-x)y^2(1-y)$$

and

$$\nu_e(x,y) = \nu_0 + (\nu_1 - \nu_0)\exp(-10^{12}((x-0.5)^{10} + (y-0.5)^{10})).$$

Moreover, we will take the following values for $\nu_0 = 0.1$ and $\nu_1 = 1$. And the stabilisation parameters as $\kappa_1 = \frac{2}{3}\nu_0$, $\kappa_2 = \frac{\nu_0}{2}$, $\sigma = 10$.

We notice that the pressure is singular near the reentrant corner of the domain and so we expect hindered convergence of the approximations when a uniform (or quasi-uniform) mesh refinement is applied. In contrast, if we apply the following adaptive mesh refinement procedure from [53]:

1) Start with a coarse mesh $\mathcal{T}_h$.
2) Solve the discrete problem (3.2) for the current mesh $\mathcal{T}_h$.
3) Compute $\Theta_T := \Theta$ for each triangle $T \in \mathcal{T}_h$.
4) Check the stopping criterion and decide whether to finish or go to next step.
5) Use *blue-green* refinement on those $T' \in \mathcal{T}_h$ whose indicator $\Theta_{T'}$ satisfies

$$\Theta_{T'} \geq \frac{1}{2} \max_{T \in \mathcal{T}_h} \{\Theta_T : \; T \in \mathcal{T}_h\} \,.$$

6) Define resulting meshes as current meshes $\mathcal{T}_h$ and $\mathcal{T}_h$, and go to step 2,

we expect a recovering of the optimal convergence rates. In fact, this can be observed from the bottom rows of Tables 5.4 and 5.5 that such optimal convergence rate is recovered for both viscosity functions ν_d and ν_e, respectively. Moreover, we note that the efficiency indexes are around 1 for both viscosity functions.

The resulting meshes after a few adaptation steps are reported in Figure 5.2. We observe intensive refinement near the reentrant corner of the domain as expected.

N	$\\|\boldsymbol{u}-\boldsymbol{u}_h\\|_{1,\Omega}$	$r(\boldsymbol{u})$	$\\|\omega-\omega_h\\|_{0,\Omega}$	$r(\omega)$	$\\|p-p_h\\|_{0,\Omega}$	$r(p)$	$\texttt{eff}(\Theta)$
381	54.13	–	10.85	–	32.21	–	4.040
489	132.2	-7.15	31.81	-8.62	35.11	-0.68	2.198
571	144.9	-1.18	41.43	-3.40	22.06	5.99	1.059
661	49.68	14.6	8.821	21.1	6.685	16.3	1.133
999	32.37	2.07	5.069	2.68	3.985	2.50	1.157
1241	15.46	6.81	2.104	8.10	1.846	7.09	1.144
1881	9.058	2.57	1.396	1.97	1.057	2.68	1.098
2103	7.178	4.17	0.907	7.72	0.828	4.36	1.135
2621	5.645	2.18	0.754	1.67	0.655	2.12	1.120
3851	3.647	2.27	0.454	2.63	0.418	2.33	1.168
4267	3.243	2.29	0.401	2.46	0.365	2.61	1.156
5271	2.687	1.77	0.298	2.76	0.294	2.03	1.143
7819	1.754	2.16	0.194	2.18	0.191	2.22	1.155

Table 5.4 Example 3: Convergence history and effectivity indexes for the mixed finite element method introduced in Section 3.1.1, computed on a sequence of adaptively refined triangulations of the L-shaped domain and viscosity ν_d.

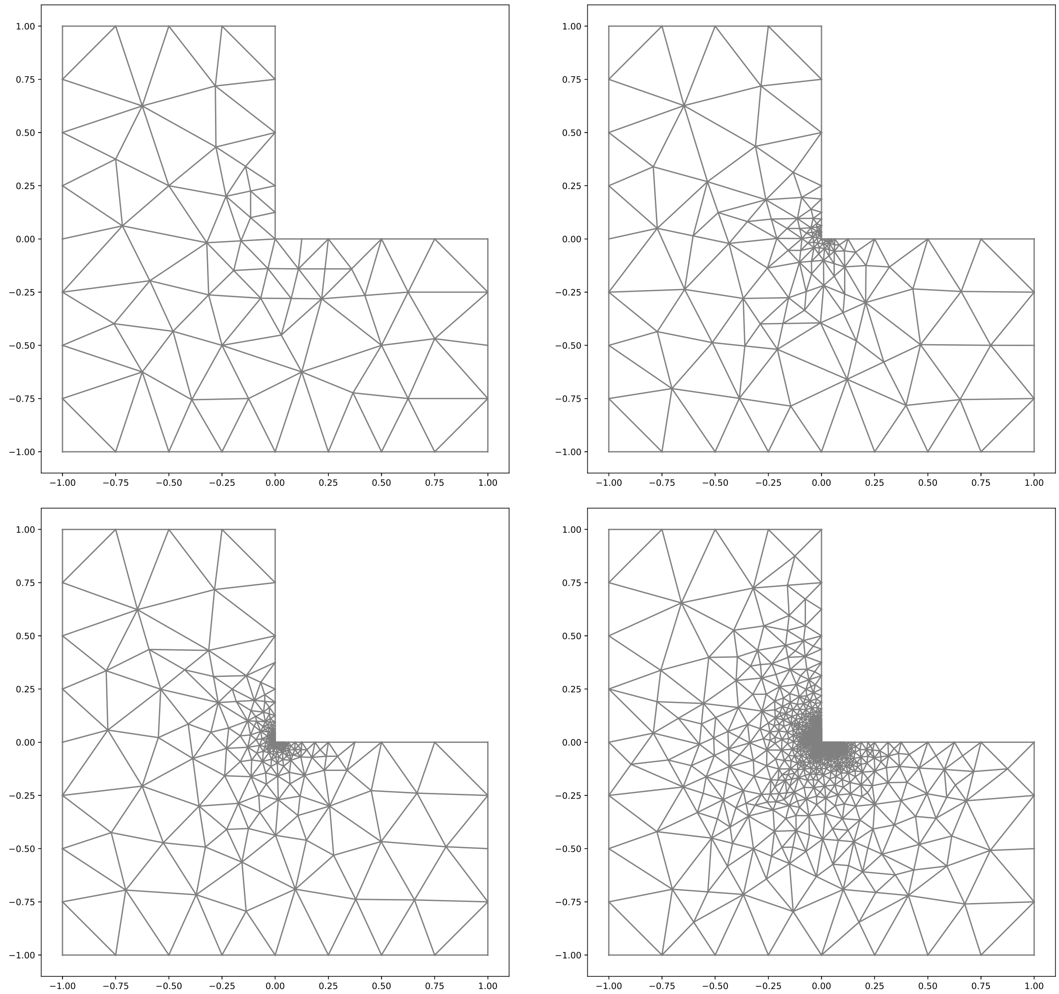

Fig. 5.2 Example 3: Snapshots of four grids, $\mathcal{T}_h^1$ (top left), $\mathcal{T}_h^4$ (top right), $\mathcal{T}_h^6$ (bottom left) and $\mathcal{T}_h^{10}$ (bottom right), adaptively refined according to the a posteriori error indicator defined in (4.1).

N	$\|\boldsymbol{u}-\boldsymbol{u}_h\|_{1,\Omega}$	$r(\boldsymbol{u})$	$\|\omega-\omega_h\|_{0,\Omega}$	$r(\omega)$	$\|p-p_h\|_{0,\Omega}$	$r(p)$	$\mathtt{eff}(\Theta)$
381	59.77	–	13.42	–	32.31	–	3.715
489	133.9	-6.46	33.24	-7.27	35.03	-0.64	2.166
571	145.2	-1.04	41.84	-2.97	22.05	5.97	1.054
661	49.73	14.6	8.842	21.2	6.681	16.3	1.132
999	32.39	2.07	5.081	2.68	3.980	2.50	1.155
1241	15.50	6.79	2.122	8.05	1.838	7.12	1.138
1881	9.087	2.56	1.401	1.99	1.039	2.74	1.085
2103	7.213	4.14	0.914	7.65	0.806	4.55	1.114
2589	5.683	2.29	0.759	1.78	0.633	2.32	1.112
3771	3.734	2.23	0.461	2.64	0.406	2.35	1.113
5161	2.674	2.12	0.307	2.58	0.287	2.20	1.108
6867	1.946	2.22	0.207	2.77	0.205	2.36	1.116
9887	1.346	2.02	0.128	2.60	0.138	2.16	1.119

Table 5.5 Example 3: Convergence history and effectivity indexes for the mixed finite element method introduced in Section 3.1.1, computed on a sequence of adaptively refined triangulations of the L-shaped domain and viscosity ν_e.

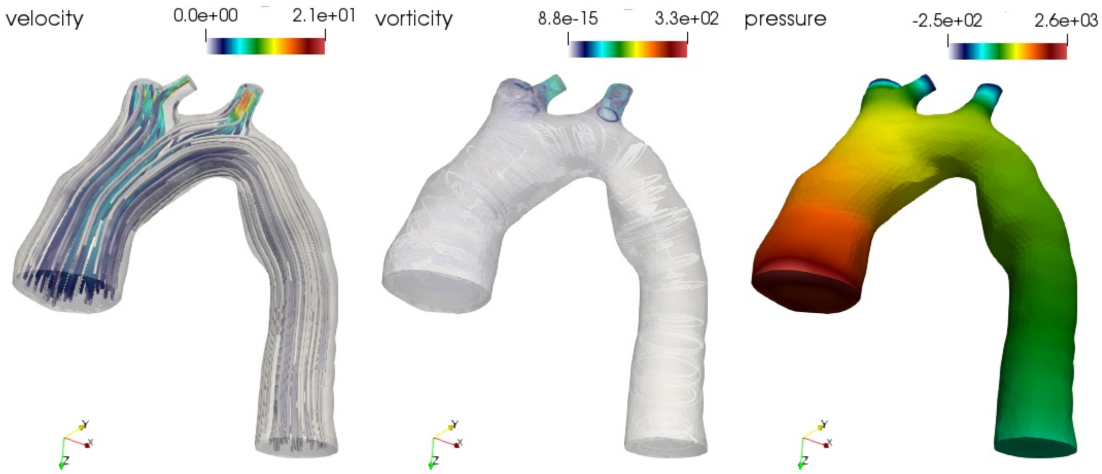

Fig. 5.3 Example 4: Approximate velocity, vorticity, and pressure for the simulation of stationary blood flow in an aortic arch.

5.4 Example 4: Steady blood flow in aortic arch

We finalise the set of examples with a simple simulation of pseudo-stationary blood flow in an aorta. The patient-specific geometry [42,43] has one inlet (a segment that connects with the pre-aortic root coming from the aortic valve in the heart) and four outlets (the left common carotid artery, the left subclavian artery, the innominate artery, and the larger descending aorta). The unstructured mesh has 46352 tetraherdal elements. On the inlet we impose a Poiseuille profile of magnitude 4, on the vessel walls we set no-slip conditions, and on the remaining boundaries we set zero normal stresses (more physiologically relevant boundary conditions can be considered following, e.g., [28,36]). The synthetic variable viscosity field is a smooth exponential function that entails an average Reynolds number of approximately 60 (computed using the inlet diameter and maximal inlet velocity), while the convecting velocity is computed as the solution of a preliminary Stokes problem. The results are portrayed in Figure 5.3, showing pressure distribution, velocity streamlines, and vorticity. For this test we have used discontinuous vorticity.

Acknowledgements This work has been partially supported by DIUBB through projects 2020127 IF/R and 194608 GI/C, by the National Agency for Research and Development, ANID-Chile, through project Centro de Modelamiento Matemático (AFB170001) of the PIA Program: Concurso Apoyo a Centros Científicos y Tecnológicos de Excelencia con Financiamiento Basal, by the Monash Mathematics Research Fund S05802-3951284, and by the HPC-Europa3 Transnational Access programme through grant HPC175QA9K.

References

1. M. Ainsworth and J.T. Oden, *A posteriori error estimation in finite element analysis.* Wiley, New York, 2000.
2. M. Amara, D. Capatina-Papaghiuc, and D. Trujillo, *Stabilized finite element method for Navier-Stokes equations with physical boundary conditions.* Math. Comp., 76(259) (2007) 1195–1217.
3. M. Amara, E. Chacón Vera, and D. Trujillo, *Vorticity–velocity–pressure formulation for Stokes problem.* Math. Comp., 73(248) (2004) 1673–1697.
4. V. Anaya, M. Bendahmane, D. Mora and R. Ruiz-Baier, *On a vorticity-based formulation for reaction-diffusion-Brinkman systems*, Netw. Heterog. Media, **13**(1) (2018), pp. 69–94.
5. V. Anaya, A. Bouharguane, D. Mora, C. Reales, R. Ruiz-Baier, N. Seloula and H. Torres, *Analysis and approximation of a vorticity-velocity-pressure formulation for the Oseen equations*, J. Sci. Comput., **88**(3) (2019) pp. 1577–1606.

6. V. Anaya, G.N. Gatica, D. Mora, and R. Ruiz-Baier, *An augmented velocity-vorticity-pressure formulation for the Brinkman equations.* Int. J. Numer. Meth. Fluids, 79(3) (2015) 109-137.
7. V. Anaya, B. Gómez-Vargas, D. Mora and R. Ruiz-Baier, *Incorporating variable viscosity in vorticity-based formulations for Brinkman equations*, C. R. Math. Acad. Sci. Paris, 357(6), (2019), 552–560.
8. V. Anaya, D. Mora, R. Oyarzúa, and R. Ruiz-Baier, *A priori and a posteriori error analysis of a mixed scheme for the Brinkman problem.* Numer. Math., 133(4) (2016) 781-817.
9. V. Anaya, D. Mora, C. Reales and R. Ruiz-Baier, *Vorticity-pressure formulations for the Brinkman-Darcy coupled problem*, Numer. Methods Partial Differential Equations, **35**(2) (2019) pp. 528–544.
10. V. Anaya, D. Mora, and R. Ruiz-Baier, *An augmented mixed finite element method for the vorticity-velocity-pressure formulation of the Stokes equations.* Comput. Methods Appl. Mech. Engrg., 267 (2013) 261–274.
11. T.P. Barrios, J.M. Cascón and M. González, *Augmented mixed finite element method for the Oseen problem: a priori and a posteriori error analyses*, Comput. Methods Appl. Mech. Engrg., **313**, (2017), pp. 216–238.
12. M. Benzi and M. A. Olshanskii, *An augmented Lagrangian-based approach to the Oseen problem.* SIAM J. Sci. Comput. (2006), 28(6):2095–2113.
13. M. Benzi, M.A. Olshanskii, L.G. Rebholz and Z. Wang, *Assessment of a vorticity based solver for the Navier–Stokes equations,* Comput. Methods Appl. Mech. Engrg., 247-248, (2012) 216–225.
14. C. Bernardi, and N. Chorfi, *Spectral discretization of the vorticity, velocity, and pressure formulation of the Stokes problem.* SIAM J. Numer. Anal., 44(2) (2006) 826–850.
15. P.V. Bochev, *Analysis of least-squares finite element methods for the Navier–Stokes equations.* SIAM J. Numer. Anal., 34(5) (1997) 1817–1844.
16. P.V. Bochev, and M. Gunzburger, *Least-Squares finite element methods.* Volume 166 of Applied Mathematical Sciences. Springer Verlag (2009).
17. D. Boffi, *Stability of higher order triangular Hood–Taylor methods for stationary Stokes equations.* Math. Models Methods Appl. Sci., 2(4) (1994) 223–235.
18. D. Boffi, *Three–dimensional finite element methods for the Stokes problem.* SIAM J. Numer. Anal., 34(2) (1997) 664–670.
19. D. Boffi, F. Brezzi, and M. Fortin, *Mixed Finite Element Methods and applications.* Springer Series in Computational Mathematics, 44. Springer, Heidelberg (2013).
20. Z. Cai and B. Chen, *Least-squares method for the Oseen equation*, Numer. Methods Partial Differential Equations, **32**, (2016), pp. 1289–1303.
21. J. Camaño, R. Oyarzúa, R. Ruiz-Baier, and G. Tierra, *Error analysis of an augmented mixed method for the Navier-Stokes problem with mixed boundary conditions*, IMA J. Numer. Anal., **38**(3), (2018), pp. 1452–1484.
22. J. Camaño, R. Oyarzúa, and G. Tierra, *Analysis of an augmented mixed-FEM for the Navier-Stokes problem*, Math. Comp., **86**(304), (2017), pp. 589–615.
23. J.O. Campos, R. Weber dos Santos, J. Sundnes, and B. Martins Rocha, *Preconditioned augmented Lagrangian formulation for nearly incompressible cardiac mechanics.* Int. J. Numer. Methods Biomed. Engrg. (2018), **34(4)**:e2948.
24. C.L. Chang, and B.-N. Jiang, *An error analysis of least-squares finite element method of velocity-pressure-vorticity formulation for the Stokes problem.* Comput. Methods Appl. Mech. Engrg., 84(3) (1990) 247–255.
25. C.L. Chang and S.-Y. Yang, *Analysis of the* $[L^2, L^2, L^2]$ *least-squares finite element method for incompressible Oseen-type problems,* Int. J. Numer. Anal. Model., 4(3-4), (2007), 402–424.
26. P. Clément, *Approximation by finite element functions using local regularisation.* RAIRO Modél. Math. Anal. Numer. 9 (1975) 77–84.
27. B. Cockburn, and J. Cui, *An analysis of HDG methods for the vorticity-velocity-pressure formulation of the Stokes problem in three dimensions.* Math. Comp., 81(279) (2012) 1355–1368.
28. T. Dobroserdova, F. Liang, G. Panasenko, and Y. Vassilevski, *Multiscale models of blood flow in the compliant aortic bifurcation.* Appl. Math. Letters 93C, 98–104, (2019).
29. H.-Y. Duan, and G.-P. Liang, *On the velocity-pressure-vorticity least-squares mixed finite element method for the 3D Stokes equations.* SIAM J. Numer. Anal., 41(6) (2003) 2114–2130.
30. F. Dubois, M. Salaün, and S. Salmon, *First vorticity-velocity-pressure numerical scheme for the Stokes problem.* Comput. Methods Appl. Mech. Engrg., 192(44–46) (2003) 4877–4907.
31. A. Ern, *Vorticity-velocity formulation of the Stokes problem with variable density and viscosity*, Math. Models Methods Appl. Sci., **8**(2), (1998), pp. 203–218.
32. A. Ern and J.-L. Guermond, Theory and Practice of Finite Elements. Applied Mathematical Sciences. Springer-Verlag, (2004).
33. P.E. Farrell, L. Mitchell, and F. Wechsung, *An augmented Lagrangian preconditioner for the 3D stationary incompressible Navier-Stokes equations at high Reynolds number.* SIAM J. Sci. Comput. (2019) **41(5)**:A3073–A3096.
34. P.E. Farrell and P.A. Gazca-Orozco, *An augmented Lagrangian preconditioner for implicitly-constituted non-Newtonian incompressible flow.* SIAM J. Sci. Comput. 42(6) (2020), B1329–B1349.
35. P.E. Farrell, L.F. Gatica, B.P. Lamichhane, R. Oyarzúa, and R. Ruiz-Baier , *Mixed Kirchhoff stress - displacement - pressure formulations for incompressible hyperelasticity.* Comput. Methods Appl. Mech. Engrg., 374 (2021) e113562.

36. L Formaggia, J.F. Gerbeau, F. Nobile, and A. Quarteroni, *Numerical treatment of defective boundary conditions for the Navier-Stokes equations.* SIAM J. Numer. Anal. 40, 376–401 (2002).
37. G.N. Gatica, *A Simple Introduction to the Mixed Finite Element Method. Theory and Applications.* Springer Briefs in Mathematics, Springer, Cham Heidelberg New York Dordrecht London (2014).
38. G.N. Gatica, R. Oyarzúa, and N. Valenzuela, *A five-field augmented fully-mixed finite element method for the Navier-Stokes/Darcy coupled problem.* Comput. Math. Appl., 80(8) (2020) 1944–1963.
39. V. Girault, and P.A. Raviart, *Finite element methods for Navier-Stokes equations. Theory and Algorithms.* Springer-Verlag, Berlin (1986).
40. P. Hood, and C. Taylor, *Numerical solution of the Navier–Stokes equations using the finite element technique.* Comput. Fluids, 1 (1973) 1–28
41. V. John, K. Kaiser, and J. Novo, *Finite element methods for the incompressible Stokes equations with variable viscosity*, ZAMM Z. Angew. Math. Mech , **96**(2), (2016), pp. 205–216.
42. E. Marchandise, P. Crosetto, C. Geuzaine, J.-F. Remacle, and E. Sauvage, *Quality open source mesh generation for cardiovascular flow simulation.* In: D. Ambrosi, A. Quarteroni, and G. Rozza, editors. Modeling of Physiological Flows. Milano: Springer (2011) 395–414.
43. E. Marchandise, E. Sauvage, and J.-F. Remacle, *Quality open source mesh generation for biological flow simulations.* In: Proceedings of the ECCOMAS Thematic International Conference on Simulation and Modeling of Biological Flows (SIMBIO 2011) September 21?23, 2011, VUB, Brussels, Belgium.
44. S. Mohapatra and S. Ganesan, *A non-conforming least squares spectral element formulation for Oseen equations with applications to Navier-Stokes equations,* Numer. Funct. Anal. Optim., 37(10), (2016), 295–1311.
45. P.R. Patil and G. Vaidyanathan, *Effect of variable viscosity on thermohaline convection in a porous medium.* J. Hydrology, 57(1-2) (1982) 147–161.
46. L.E. Payne, J.C. Song, and B. Straughan, *Continuous dependence and convergence results for Brinkman and Forchheimer models with variable viscosity.* Proc. Royal Soc. London Series A, 455 (1986) 1–20.
47. J.P. Pontaza, and J.N. Reddy, *Spectral/hp least-squares finite element formulation for the Navier-Stokes equations.* J. Comput. Phys., 190(2) (2003) 523–549.
48. J. Rudi, G. Stadler, and O. Ghattas, *Weighted BFBT preconditioner for Stokes flow problems with highly heterogeneous viscosity.* SIAM J. Sci. Comput., 39(5) (2017) S272–S297.
49. M. Salaün, and S. Salmon, *Numerical stabilization of the Stokes problem in vorticity-velocity-pressure formulation.* Comput. Methods Appl. Mech. Engrg., 196(9-12) (2007) 1767–1786.
50. M. Salaün, and S. Salmon, *Low-order finite element method for the well-posed bidimensional Stokes problem.* IMA J. Numer. Anal., 35 (2015) 427–453.
51. C.G. Speziale, *On the advantages of the vorticity-velocity formulations of the equations of fluid dynamics.* J. Comput. Phys., 73(2) (1987) 476–480.
52. C.-C. Tsai and S.-Y. Yang, *On the velocity-vorticity-pressure least-squares finite element method for the stationary incompressible Oseen problem,* J. Comput. Appl. Math., 182(1), (2005), 211–232.
53. R. Verfürth, *A review of a posteriori error estimation and adaptive-mesh-refinement techniques.* Wiley-Teubner, Chichester (1996).